[redacted]

CYCLOTRON RESEARCH

UNIVERSITY OF WASHINGTON

ANNUAL PROGRESS REPORT 1963

U. S. ATOMIC ENERGY COMMISSION
CONTRACT A.T. (45-1)-1388

UNIVERSITY OF WASHINGTON

Department of Physics

Cyclotron Research

PROGRESS REPORT FOR YEAR ENDING JUNE 15, 1963

PROGRAM "A"--EXPERIMENTAL PHYSICS PROGRAM (CYCLOTRON)

UNDER

U.S. ATOMIC ENERGY COMMISSION CONTRACT A.T. (45-1)-1388

PREFACE

This report reviews the research and technical development conducted at the Nuclear Physics Laboratory of the University of Washington during the year ending June 15, 1963.

The investigations described in this report, for the most part, continue and extend experimental work described in several earlier reports. Notable among these are the studies of alpha particle scattering, which have been extended to elements as heavy as Ytterbium and Zirconium; the study of alpha particle and proton scattering from gaseous targets; the continued study of the spectra of neutrons and charged particles emitted by compound nuclei; and the study of direct interaction processes which have been extended to the pickup of alpha particles, both by deuterons and by alpha particles.

Research at this laboratory is performed by the faculty and graduate students of the Departments of Physics and Chemistry of the University of Washington. Support for this project is provided by the State of Washington, the U.S. Atomic Energy Commission, and the National Science Foundation.*

The arrangement of this report follows the pattern used in previous years. The sections are numbered consecutively through the report; each table and figure is assigned the number of the section to which it pertains. As has been our practice, the names of investigators listed at the end of each section are given in strict alphabetical order.

---

*The National Science Foundation has provided funds for the purchase of the Van de Graaff accelerator and some of its associated equipment and, in part, for the building to house the new accelerator.

TABLE OF CONTENTS

I. BETA AND GAMMA RAY SPECTROSCOPY

1. 4.1 MeV Positron Spectrum of O^{14}

The investigation of the high-energy positron spectrum of O^{14}, mentioned in earlier reports,[1] has been continued during the past year. The O^{14} source was obtained by freezing H_2O^{14} at the end of a copper rod cooled by liquid nitrogen. A NaI(Tl) scintillation counter was used to monitor the O^{14} activity at the source position of the β-ray spectrometer and an end-window Geiger counter was used as a detector of positrons.

Initial Kurie plots obtained from the data with the above equipment appeared to yield substantial deviations from linearity. This would normally be interpreted as a momentum dependence in the shape factor for the allowed 4.1 MeV positron spectrum. To ascertain whether the deviations were due to genuine second-order effects or were instrumental in origin, a study of the high-energy positron branch of Ga^{66} was made. Since O^{14} and Ga^{66} have the same end-point energies to closer than 1% and the shape of Ga^{66} positron spectrum is now accurately known,[2] the latter is suitable to detect any distortion due to source backing, calibration, etc. Ga^{66} was produced by bombarding natural Zn foils with protons from the cyclotron. With thin backing, the spectrum shape was found to agree with that found by Camp and Langer,[2] within statistical error. But on making the source backing and other conditions similar to those used for O^{14}, considerable deviations from linearity were observed. Presumably the elastic scattering of positrons from copper nuclei, at large angles, causes this distortion. The observed deviation of the thick-backing spectrum from the thin-backing spectrum is as large as 20% at low momentum values (see Fig. 1-1). If the observed distortion correction is applied to the spectrum of O^{14}, one could, in principle, obtain the true shape factor for this decay. To do so will require improvement of the statistical accuracy of the experiment by an order of magnitude. The data obtained for determination of the spectrum shape were used to make a rough estimate of the branching ratio of Fermi and Gamow-Teller decays of O^{14}. Since the observed spectra were not the true spectra, the values obtained are only tentative. By picking the best spectra and using their linear portions, a value of about 0.4% was obtained for the branching to the 4.1 MeV ground-state transition. (J. B. Gerhart and G. S. Sidhu)

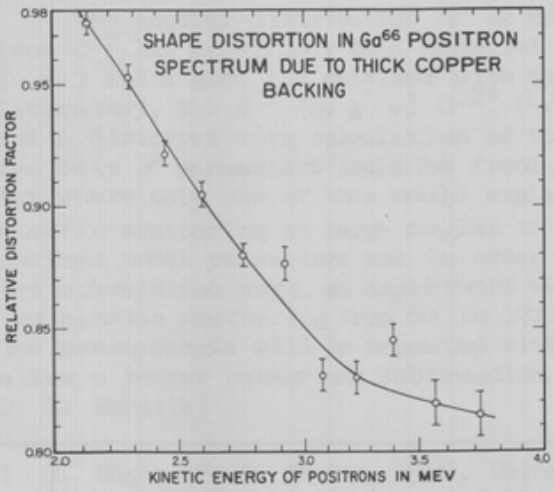

Fig. 1-1

Relative distortion of Ga^{66} spectrum because of thick source backing (arbitrary normalization).

1 Cyclotron Research, University of Washington (1962), p. 2; (1961), p. 2; (1959), p. 5.
2 D. C. Camp and L. M. Langer, Phys. Rev. 129, 1782 (1963).

2. Carbon - 10 and the Cluster Model

The studies of the C^{10} spectrum reported last year have now been completed.[1] A calculation, based upon the so-called cluster model, leads to a predicted value for the end-point of the C^{10} spectrum of 3.52 MeV. The measured value is 4.61 MeV. Hence, we conclude that the cluster model is inconsistent with experimental evidence in its description of the spatial properties of these nuclear clusters. (F. J. Bartis and F. H. Schmidt)

1 F. J. Bartis and F. H. Schmidt, Bull. Am. Phys. Soc. 7, 461 (1962).

II. NUCLEAR SCATTERING AND CORRELATIONS OF SCATTERED PARTICLES WITH GAMMA RAYS

3. Inelastic Scattering of Alpha Particles from a 14 MeV Level in C^{12}

The angular distribution of inelastically scattered alpha particles corresponding to a level around 14 MeV in C^{12} is being measured. This 14 MeV level could be the 4^+ level of the rotational band; 0^+, 2^+ (4.43 MeV). Preliminary data show (Fig. 3 - 1): (1) no forward peak, which qualitatively favors a double excitation process; (2) a relatively high cross section at large angles (comparable to the 4.43 MeV level), which again favors a double excitation process; (3) no agreement with the phase rules, which can be explained by the fact that we are now far away (14 MeV excitation) from the adiabatic approximation conditions.

Qualitatively, there is no contradiction with the "coupled channel calculations" made by Wills[1] for the angular distribution of an $0^+ \rightarrow 4^+$ double excitation process. (J. Alster, D. Garreta, D. L. Hendrie, R. J. Peterson)

---

1 J. Wills, Ph.D. Thesis, University of Washington, 1963 (unpublished).

---

4. Elastic Scattering of 42 MeV Alpha Particles from C^{12} at Large Angles

The angular distribution of 42 MeV alpha particles elastically scattered from C^{12} has previously been measured in this laboratory from 15 to 80 deg. (c.m.) and a good fit obtained with the Blair diffraction model.[1] Also in this laboratory, the C^{12} $(\alpha, \alpha' \gamma)$ C^{12*} (4.43) alpha-gamma correlation was measured, and a distorted wave calculation of the correlation pattern was performed where two sets of parameters could be found that would fit the elastic scattering data, but where only one of them could explain the correlation function.[2] Since the elastic scattering at large angles is important for finding a unique set of optical model parameters and in order to check the optical potential found from the correlation work, an experiment was started to measure, with good statistics, the elastic scattering from 60 to 170 deg. (lab). Preliminary data were obtained. The measurements will be repeated with a thinner and oxygen-free target that will allow a better background subtraction. (J. Alster, A. Bernstein, G. W. Farwell, D. L. Hendrie)

---

1 I. Naqib, Ph.D. Thesis, 1962, University of Washington (unpublished).

2 R. H. Bassel, D. L. Hendrie, D. K. McDaniels and G. R. Satchler, Phys. Letters 1, 295 (1962).

---

5. Inelastic Scattering of Protons by Nitrogen

The experimental work on the inelastic scattering of 10.5 MeV protons by N^{14} has been completed. The initial phase of this work was reported in last year's progress report[1] in which the experimental technique and the astrophysical

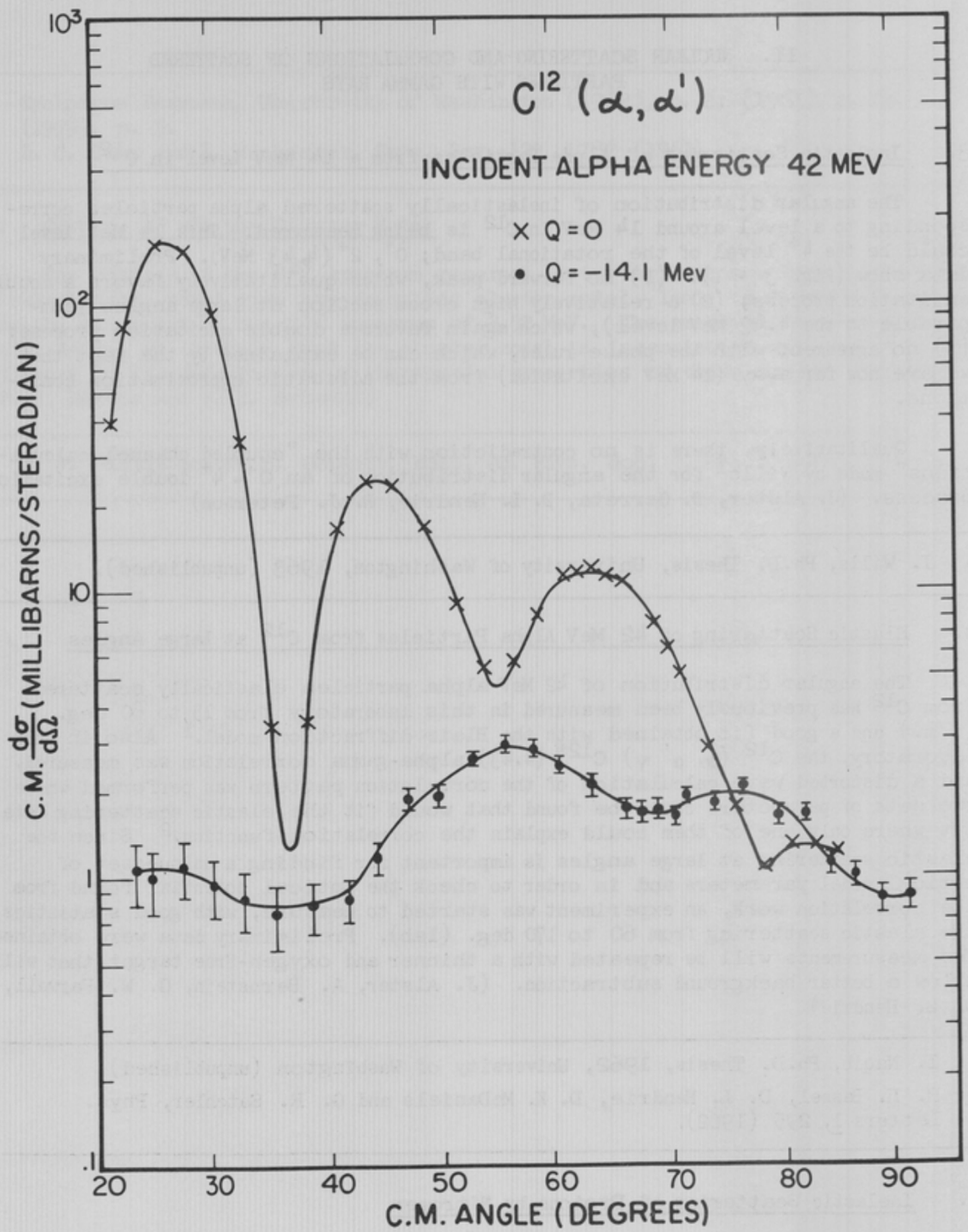

Fig. 3-1

Angular distribution for inelastic scattering of 42 MeV alpha particles from a 14 MeV level in C^{12}.

motivation for the experiment were described. A discussion of the fact that no energy levels are observed in the astrophysically important region of 7.6 MeV excitation in N^{14} has subsequently been published.[2] The observed pulse-height spectrum produced in the solid state detector set at 35° to the incident proton beam is given in Fig. 5-1. It is clear that no proton groups are observed near 7.6 MeV excitation in N^{14}.

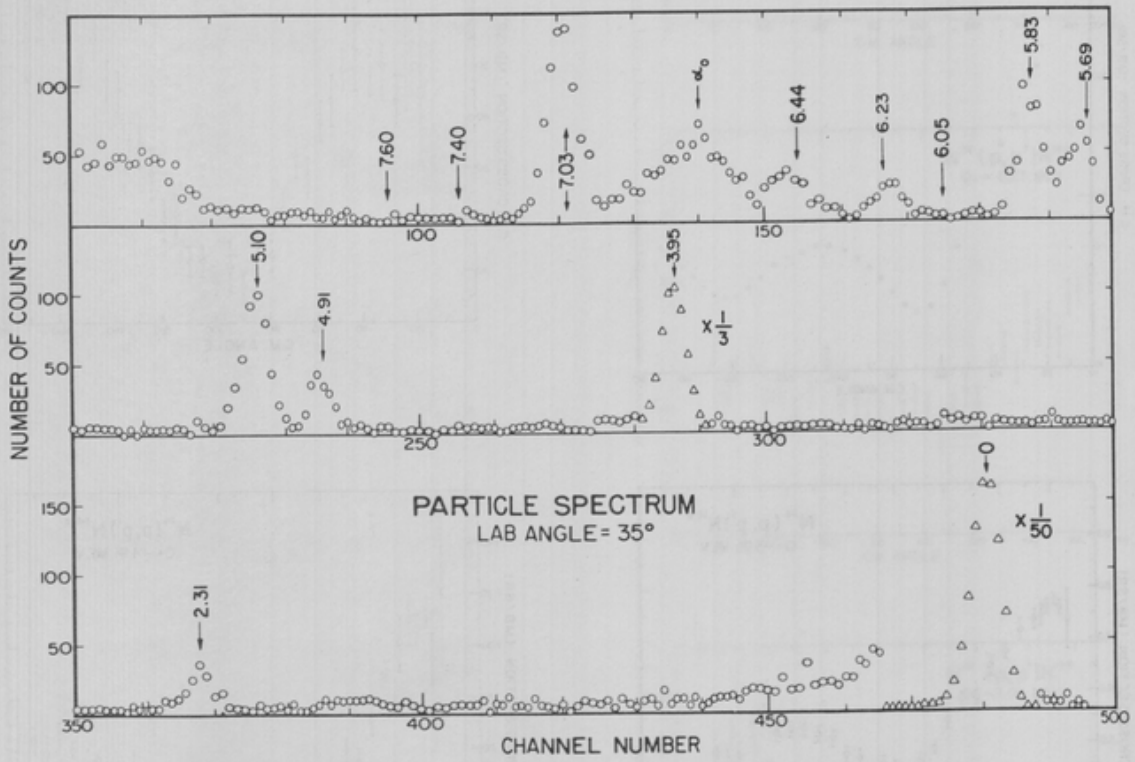

Fig. 5-1

Pulse-height spectrum produced in the solid state detector when nitrogen gas is bombarded with 10.5 MeV protons. The numbers refer to the excitation energy in MeV produced in N^{14} by the indicated proton group. α refers to the alpha-particle group from the reaction $N^{14}(p, \alpha)C^{11}$.

Angular distributions for scattered protons leading to the first ten observed states in N^{14} have been obtained. These distributions are shown (in the c.m. system) in Fig. 5-2 and 5-3. The cross sections were calculated from the

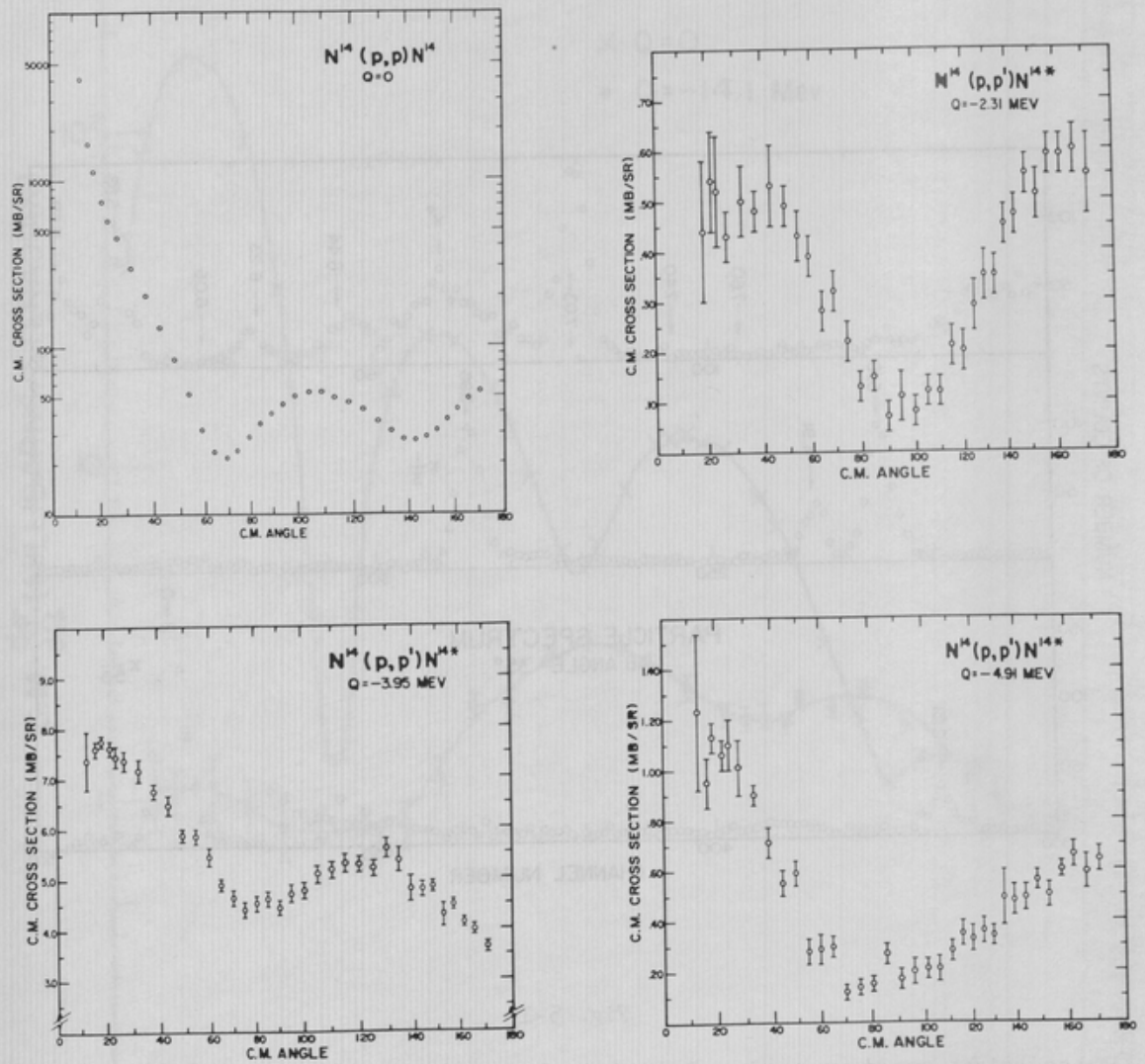

Fig. 5-2

Measured differential cross sections in the c.m. system for $N^{14}(p, p)N^{14*}$ The Q-value is as indicated.

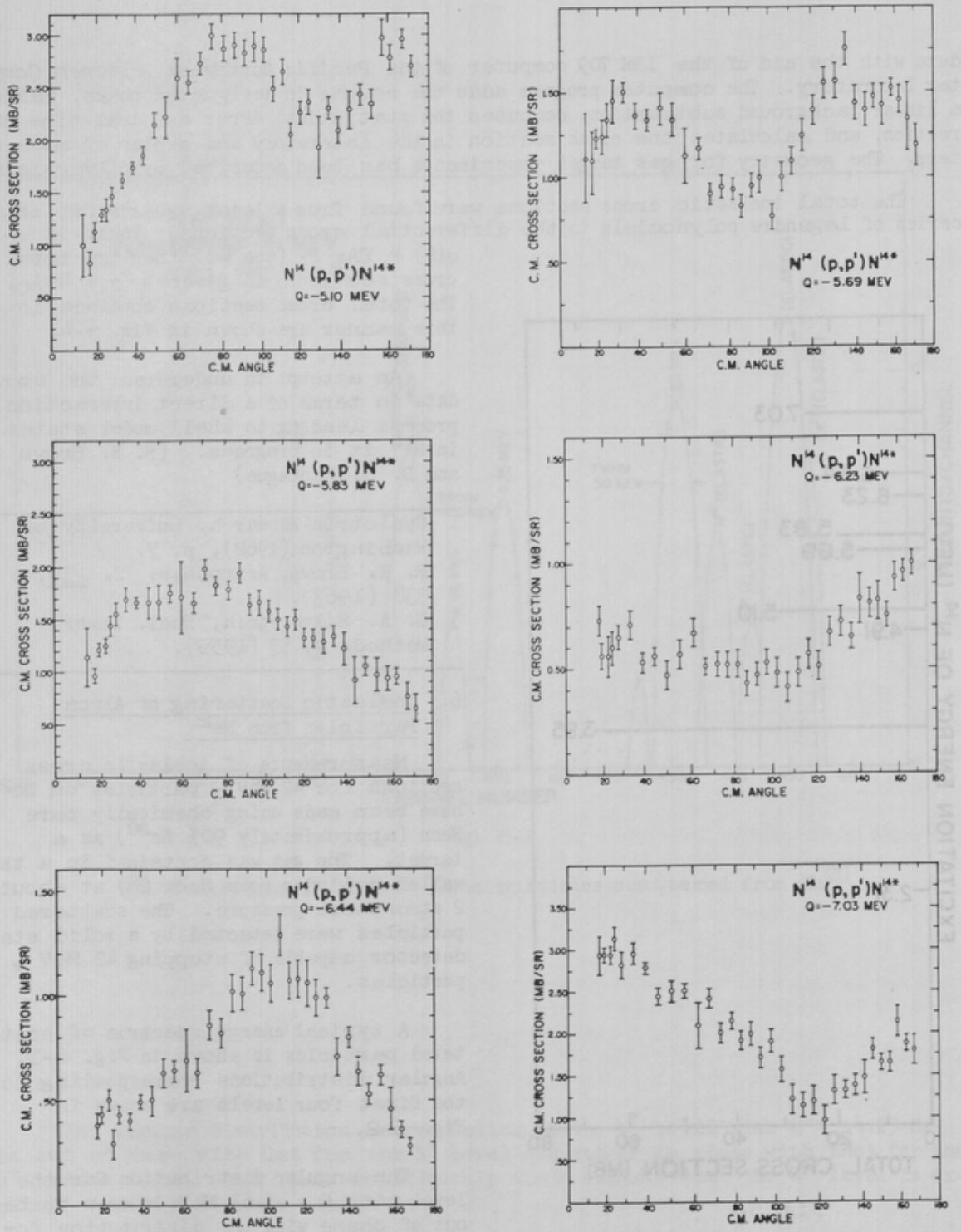

Fig. 5-3

Measured differential aross sections in the c.m. system for $N^{14}(p,p)N^{14*}$. The Q-value is as indicated.

data with the aid of the IBM 709 computer of the Pacific Northwest Research Computer Laboratory. The computer program adds the counts in designated peaks, makes a linear background subtraction, computes the statistical error and dead time correction, and calculates the cross section in the laboratory and center of mass systems. The geometry for gas target experiments has been described by Silverstein.[3]

The total inelastic cross sections were found from a least squares fit of a series of Legendre polynomials to the differential cross sections. Thus, if $\sigma(\theta) = \Sigma A_L P_L(\cos\theta)$, then the total cross section σ is given by $\sigma = 4\pi A_0$. The total cross sections obtained in this manner are shown in Fig. 5-4.

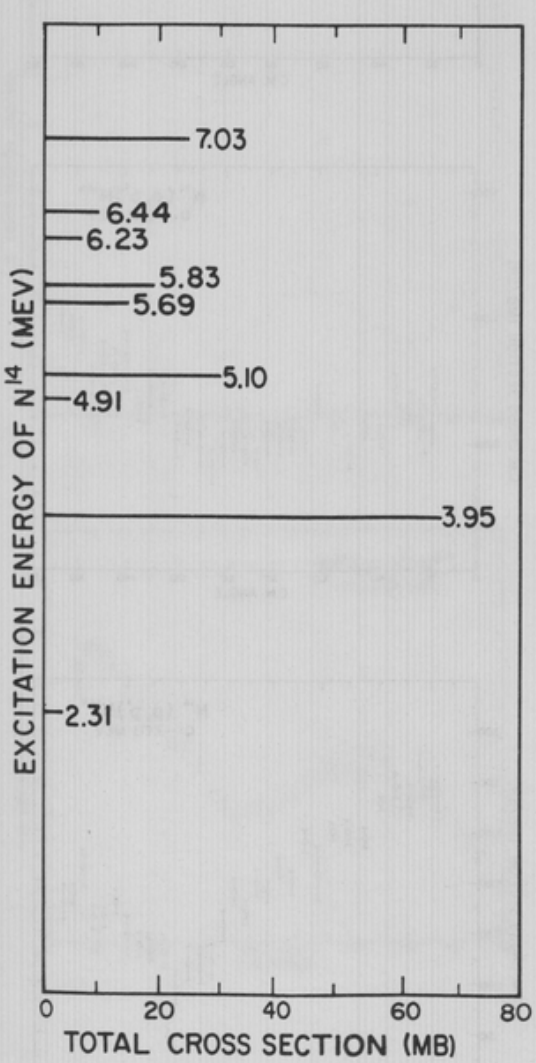

Fig. 5-4

Total cross sections for excitation by 10.5 MeV protons of the indicated states in N^{14}.

An attempt to understand the above data in terms of a direct interaction process leading to shell model states in N^{14} is in progress. (R. E. Brown and D. G. Montague)

1 Cyclotron Research, University of Washington (1962), p. 7.
2 R. E. Brown, Astrophys. J. 137, 338 (1963).
3 E. A. Silverstein, Nucl. Instr. Methods 4, 53 (1959).

6. Inelastic Scattering of Alpha Particles from Ne^{20}

Measurements of inelastic cross sections for 42 MeV α particles on Ne^{20} have been made using chemically pure Neon (approximately 90% Ne^{20}) as a target. The gas was contained in a thin-walled cylinder (see Sec. 28) at about 2 atmosphere pressure. The scattered particles were detected by a solid state detector capable of stopping 42 MeV α particles.

A typical energy spectrum of scattered particles is shown in Fig. 6-1. Angular distributions corresponding to the first four levels are shown in Fig. 6-2.

The angular distribution for the level with Q = -1.63 MeV is seen to be out of phase with the distribution for elastic scattering to the 0^+ level as predicted by the Blair phase rule.

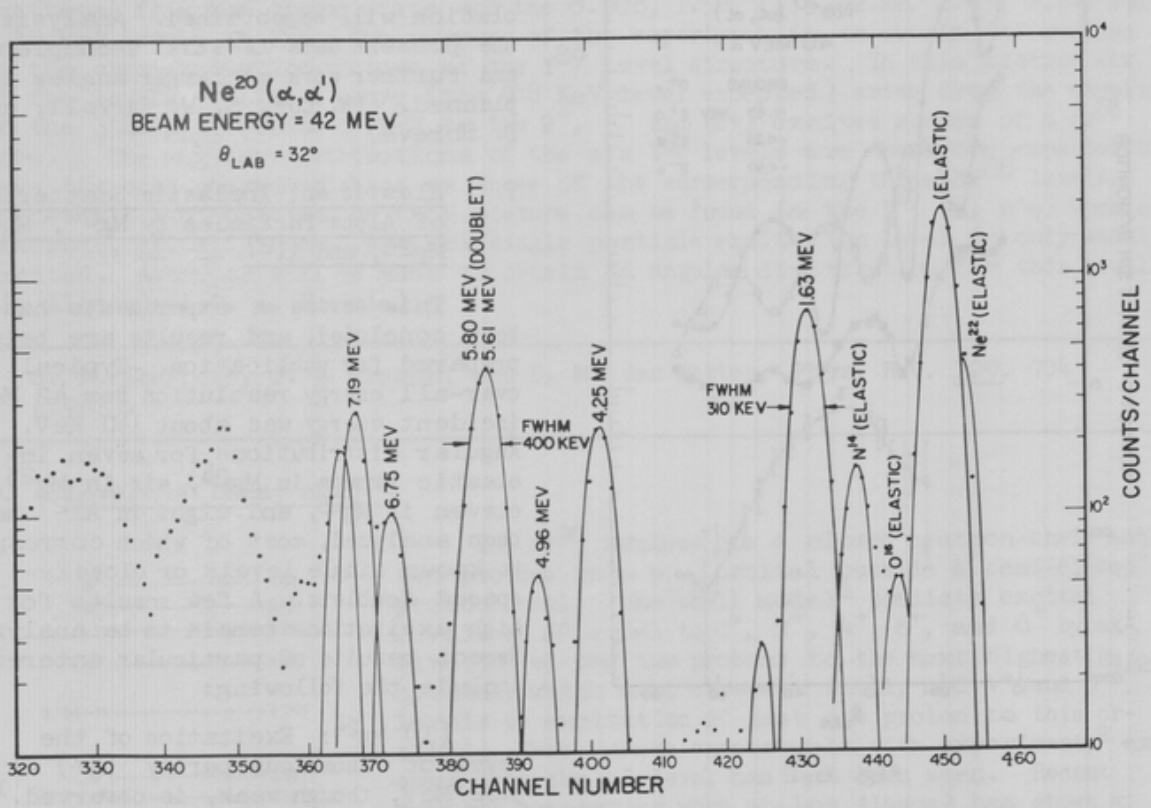

Fig. 6-1

Pulse spectrum of 42 MeV alpha particles scattered from Ne^{20}

The angular distribution corresponding to the 4^+ level with Q = -4.25 MeV is out of phase with that for the 2^+ level and rather in phase with that for the 0^+ ground state. This phase relationship would suggest that the 4^+ level is excited through a 2 phonon excitation.

The 2^- level at 4.97 MeV is only weakly excited due to its unnatural parity. Due to large backgrounds at small angles, the angular distribution is plotted for angles larger than 25°. The angular distribution is relatively free from oscillations in the region plotted and quite unlike the other levels plotted. The

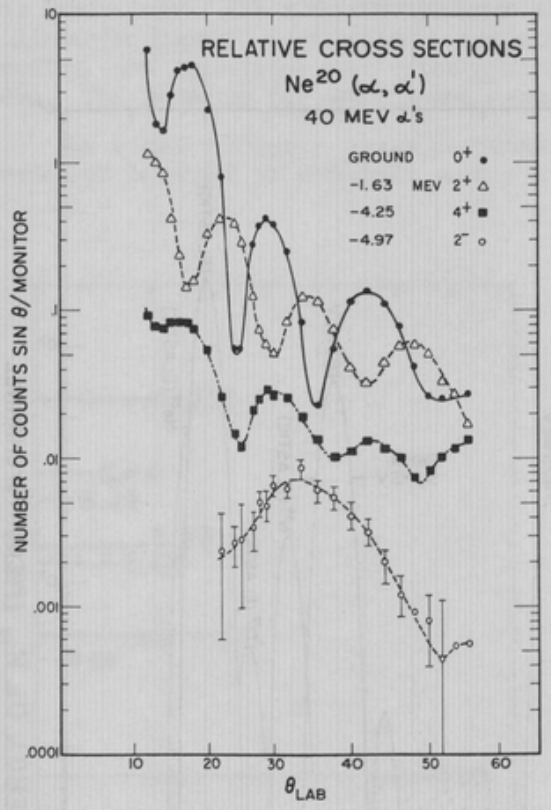

Fig. 6-2

Relative differential cross sections for scattered alpha particles corresponding to the lowest four states of of Ne^{20}.

doublet at 5.7 MeV was not resolved, but it is hoped that with thinner windows and lower pressure better resolution will be obtained. Analysis of the present data is still incomplete, and further work at larger angles is planned. (N. Cue, G. W. Farwell, and D. Shreve)

7. Elastic and Inelastic Scattering of Alpha Particles by Mg^{24}, Mg^{25}, Mg^{26}, and Al^{27}.

This series of experiments has been concluded, and results are being prepared for publication. Typical over-all energy resolution for 42 MeV incident energy was about 140 KeV. Angular distributions for seven inelastic groups in Mg^{24}, six in Mg^{25}, eleven in Mg^{26}, and eight in Al^{27} have been analyzed, most of which correspond to known single levels or closely-spaced doublets. A few results for high excitations remain to be analyzed. Recent results of particular interest include the following:

(1) Mg^{24}: Excitation of the level of "anomalous parity" (3+) at 5.22 MeV, though weak, is observed.[1]

(2) Mg^{26}: Angular distributions for the levels at 2.94 MeV (2+'), 3.58 MeV (0+), and the contributing members of the triplet near 4.33 MeV exhibit the characteristics of single-phonon excitations (ℓ = 2, 0, and 4 respectively); these results disfavor a vibrational-model interpretation of the low-lying Mg^{26} levels. The (3+) assignment for the level at 3.94 MeV is supported by strong inhibition of the corresponding inelastic alpha group which is, however, observed.[2]

(3) Al^{27}: New levels are established at 7.26 $\pm$ 0.03, 7.50 $\pm$ 0.06, and 8.00 $\pm$ 0.06 MeV. The experimental results suggest that these states are of octupole character[2, 3]. (G. W. Farwell, D. L. Hendrie, I. M. Naqib)

---

1 I. M. Naqib, Ph.D. Thesis, University of Washington, 1962 (unpublished).
2 I. M. Naqib and G. W. Farwell, Bull. Am. Phys. Soc. 8, 318 (1963).
3 G. W. Farwell, D. L. Hendrie, and I. M. Naqib, Bull. Am. Phys. Soc. 7, 454 (1962).

8. Inelastic Scattering of 42 MeV Alpha Particles from Y^{89}

Preliminary angular distributions were obtained for 42 MeV alpha particles scattered from the ground state and the 0.908, 1.51, 1.75, 2.22, 2.53, 2.84, and 3.05 MeV levels in Y^{89}. The purpose of the experiment is to obtain information on the core-excitation picture of the Y^{89} level structure. In this picture six of the levels mentioned above (the 908 KeV level excepted) arise from the coupling of the 39^{th} $p_{1/2}$ proton of Y^{89} to the 2^+, 3^- and (2+) excited states of a Sr^{88} core. The angular distributions of the six Y^{89} levels are therefore expected to have the same characteristics as those of the corresponding three Sr^{88} levels. A possible manifestation of this picture can be found in the Y^{89} (n, n'γ) work of Shafroth, et. al.[1] The 0.908 MeV single particle excitation level is only weakly excited. Attempts will be made to obtain an angular distribution for this level. (J. Alster and D. L. Hendrie)

---

1 S. M. Shafroth, P. N. Trehan, and D. M. Van Patter, Phys. Rev. 129, 704 (1963).

---

9. Levels of Decay of Zr^{90}

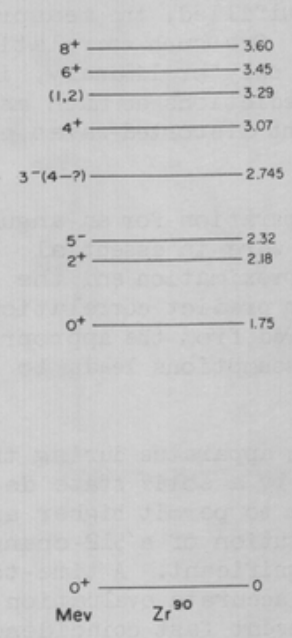

Fig. 9-1

Energy levels of Zr^{90}. The indicated branching ratios are those of reference 3.

The Zr^{90} nucleus has a closed neutron-shell and two protons in a $p_{1/2}$ orbital outside a semi-closed proton shell. The shell model[1] predicts excited levels of J^π equal to 0^+, 2^+, 4^+, 6^+, and 8^+ by excitation of the two protons to the next highest $g_{9/2}$ orbital, which also closes a shell, and 4^- and 5^- levels by excitation of just one proton to this orbital. This scheme agrees well with experiment,[2] except that the 4^- level has not been seen. Recent neutron scattering work at Los Alamos[3] has shown a strong gamma transition from a state at about 2.75 MeV to the 5^- state at 2.32 MeV. They conclude that this gamma ray comes from the missing 4^- level, which lies very close to the known 3^- collective level at 2.745 MeV.

In contrast to neutron scattering, which appears to excite all levels, inelastic alpha scattering preferentially excites levels of a collective nature. With alpha particle excitation, only the 3^- state at 2.745 MeV should be excited. A difference in the branching ratio from this level to the 2^+ and 5^- states from that of reference[3] would confirm the existence of a second level at that energy. An attempt to determine this ratio by present techniques has proven inconclusive, and further work has been postponed until improvements have been made in the apparatus and a better target is received from Oak Ridge. (J. Alster, G. W. Farwell, and D. L. Hendrie)

1 K. W. Ford, Phys. Rev. 98, 1516 (1955).
2 B. F. Bayman, A. S. Reiner, and R. K. Sheline, Phys. Rev. 115, 1627 (1959).
3 R. T. Wagner, E. R. Shunk, and R. B. Day (to be published), and R. B. Day (private communication).

10. Alpha-Gamma Angular Correlations

Alpha-gamma angular correlation measurements are being extended to elements other than carbon. Previous measurements on the 4.43 MeV 2^+ state of C^{12} have shown[1,2] strong deviations from the predictions of plane-wave Born and adiabatic[3] approximations. These theories predict correlation functions in the scattering plane of the form $\sin^2 2(\theta_\gamma - \theta_0)$, where θ_γ is the gamma detector angle, and θ_0 is either the actual or the adiabatic recoil axis. The carbon data have shown that θ_0 actually rotates in the scattering plane, agreeing with the above theories only near maxima of the inelastic differential cross section. It was further found that an isotropic component of the radiation exists near minima of the differential cross section.

To test whether either the adiabatic or plane-wave predictions are more reliable when the conditions for their validity are better fulfilled, the measurements have been extended to the 1.37 MeV 2+ state of Mg^{24}. One such correlation pattern is shown in Fig. 10-1. Results to date, which are only preliminary, indicate that the symmetry axis does not deviate from the predictions as much as was found for carbon. This is in agreement with some recent distorted-waves calculations[4].

An angular distribution on Ca^{40} has been taken in preparation for an angular correlation measurement on the 3.78 MeV 3^- level. Results were in essential agreement with those of Saudinos[5]. The plane-wave Born approximation and the diffraction model[6] extension of the adiabatic approximation predict correlation patterns of the form $(1-5\cos^2\theta_\gamma)\sin^2\theta_\gamma$ where θ_γ is measured from the appropriate nuclear recoil axis. Nonvalidity of either of these assumptions leads to correlation patterns of more complexity.

Several improvements have been made in the correlation apparatus during the past year. Replacement of the scintillation alpha counter by a solid state detector, improvement of the gamma counter electronics system to permit higher and fluctuating counting rates without gain shifts, and substitution of a 512-channel analyzer for the previous 20-channel analyzer have been significant. A time-to-pulse-height converter system is now being tested for more accurate evaluation of accidental coincidences and possible replacement of the present fast coincidence system. (J. Alster, G. W. Farwell, D. Garreta, D. L. Hendrie)

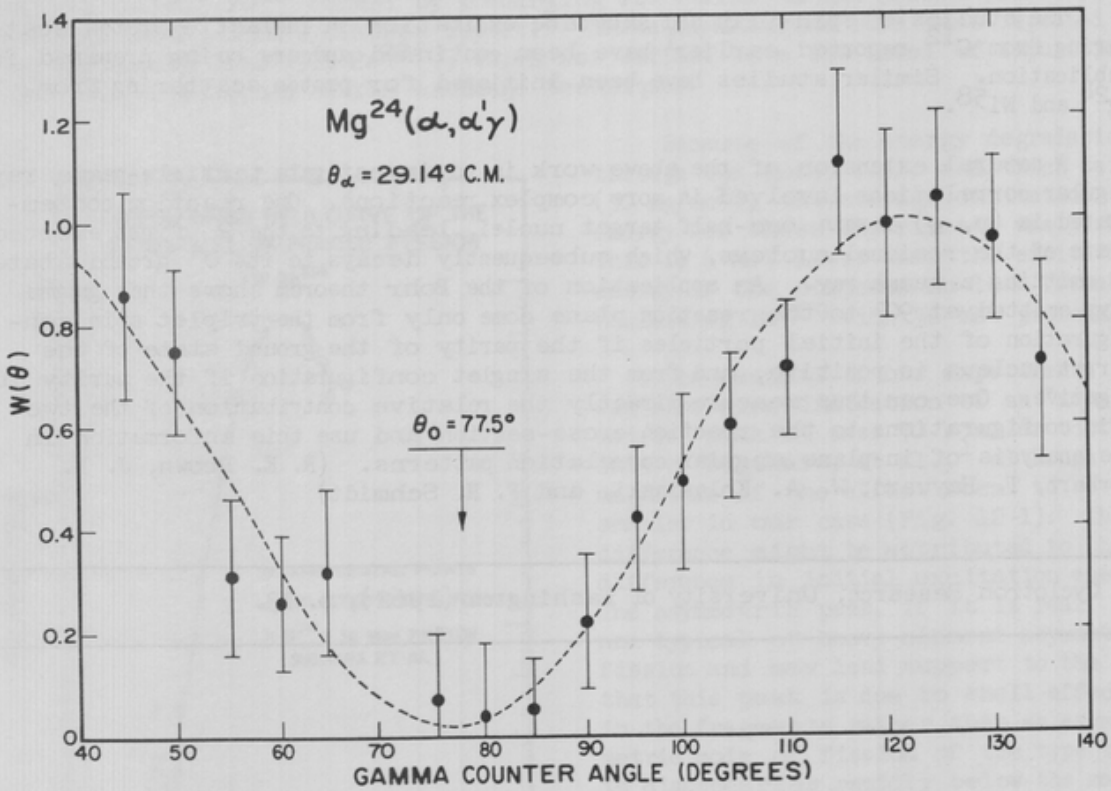

Fig. 10-1

Correlation Function $w(\theta)$ between inelastically scattered alpha particles and de-excitation gamma rays from the 1.37 MeV 2+ state of magnesium-24. The alpha angle was 25° in the laboratory system, corresponding to 29.14° in the center-of-mass system. The dotted line is a least squares fit to the data.

1 Cyclotron Research, University of Washington (1962), p. 9.
2 D. K. McDaniels, D. L. Hendrie, R. H. Bassell, and G. R. Satchler, Phys. Letters 1, 295 (1962).
3 J. S. Blair and L. Wilets, Phys. Rev. 121, 1493 (1961).
4 J. G. Wills, private communication.
5 Jean Saudinos, Ph.D. Thesis, Centre d'Etudes Nucleaires de Saclay, C.E.A. Report No. 2146 (1962).
6 J. S. Blair, Phys. Rev. 115, 928 (1956).

11. Angular Correlations of Gamma Rays with Scattered Protons

The studies of spin-flip and substate excitation in inelastic proton scattering from C^{12} reported earlier[1] have been continued and are being prepared for publication. Similar studies have been initiated for proton scattering from Mg^{24} and Ni^{58}.

A natural extension of the above work is to investigate particle-gamma ray angular correlations involved in more complex reactions. One reaction contemplated is (p, α) on spin one-half target nuclei, leading to the 2^+ first excited state of the residual nucleus, which subsequently decays to its 0^+ ground state by emitting a gamma ray. An application of the Bohr theorem shows that gamma rays emitted at 90° to the reaction plane come only from the triplet spin configuration of the initial particles if the parity of the ground state of the target nucleus is positive, and from the singlet configuration if the parity is negative. One can thus measure directly the relative contribution of the two spin configurations to the reaction cross-section and use this information in the analysis of in-plane angular correlation patterns. (R. E. Brown, J. B. Gerhart, T. Hayward, W. A. Kolasinski, and F. H. Schmidt)

1 Cyclotron Research, University of Washington (1962), p. 13.

12. Fission Study of Pb^{206}

An asymmetric fission mode has been reported to exist in the fission of Bi^{209} with 36 MeV protons.[1] This fission mode correlates strongly with magic numbers N = 52 and Z = 50, although the evidence for this fission mode comes from observations on the complimentary light fragments in the region of zinc. It seemed worthwhile to obtain further information on this development.

Previous attempts to obtain information on the asymmetric fission of the compound nucleus Po^{210} formed by bombarding Pb^{206} with 42 MeV helium ions were described in the 1962 cyclotron report.[2] These experiments have been repeated with radiogenic lead (90% Pb^{206}), which was refined to a low level of impurities by electrorefining and cation exchange techniques.

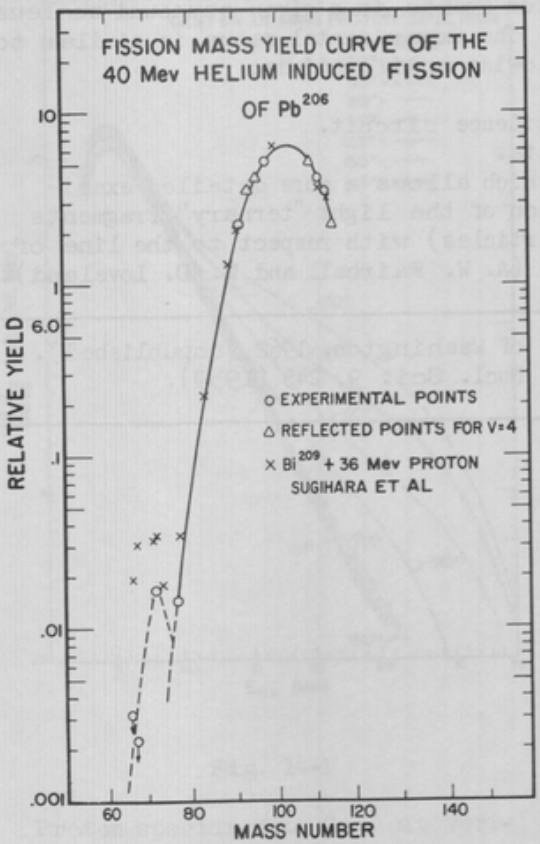

Fig. 12-1

Mass Yield curve for fission of Pb^{206} induced by 42 MeV helium ions.

Because of the energy degradation through the guard foils and thick target (50 mg/cm^2), the average excitation energy for these experiments was 35 MeV. This is 6 MeV lower than the excitation energy of the compound nucleus formed by bombarding Be^{209} with 36 MeV protons.[1]

The results of our experiments so far show some indication of an "asymmetric" peak at mass 70 similar to the data of Sugihara, et al.,[1] although the magnitude of the effect seems to be smaller in our case (Fig. 12-1). This difference might be attributed to the difference in initial excitation energy. The asymmetric peak, if it is real, is not typical of heavy element asymmetric fission and may lend support to the idea that this peak is due to shell effects in the fragments rather than an asymmetric mode of fission of the type that is disappearing rapidly below the mass region of radium. More data must be obtained before the "peak" can be established with certainty. (A. W. Fairhall and R. L. Watters)

---

1 T. T. Sugihara, J. Roesmer, and J. W. Meadows, Jr., Phys. Rev. 121, 1179 (1961).

2 Cyclotron Research, University of Washington (1962), p. 26.

13. Further Studies of Ternary Fission at Moderate Excitation Energies

Coleman has reported[1] that the relative probability of ternary fission as compared to binary fission is anomalously high for the 42 MeV alpha particle induced ternary fission of U^{238} and Th^{232} in comparison with trends seen in spontaneous and slow neutron induced fission. It was suggested that this effect may be due to the larger angular momentum of the compound nucleus in the $U^{238} + \alpha$ and $Th^{232} + \alpha$ experiments. If ternary fission studies are to be of any value in the interpretation of scission point phenomena, this possible angular momentum dependence of ternary fission must be carefully investigated.

Work is now in progress on experiments designed to examine the effect of angular momentum on the relative probability for ternary fission. Since it is fairly well established for charged particle induced fission at moderate excitation energies[2] that the more angular momentum a compound nucleus possesses, the more the fission fragment distribution will be peaked forward and backward with respect to the incident beam, examination of ternary fission events in which the heavier fission fragments are emitted at various angles with respect to the beam will correspond to examining ternary fission events in a given compound nucleus with varying amounts of angular momentum. The experimental setup is similar to that of Coleman,[1] but it includes the following modifications:

(1) A new simplified fast-slow coincidence circuit.
(2) Two-parameter analysis of the data.
(3) A new target-detector geometry which allows a more detailed examination of the angular distribution of the light "ternary" fragments (in reality, long-range alpha particles) with respect to the line of centers of the heavy fragments. (A. W. Fairhall and W. D. Loveland)

---

1 J. A. Coleman, Ph.D. Thesis, University of Washington, 1962 (unpublished).
2 See, for example, I. Halpern, Ann. Rev. Nucl. Sci. 9, 245 (1959).

---

14. Spectra and Angular Distribution of Protons Emitted in Alpha Particle Bombardments

The study of protons emitted from the isotopes of Ni (Ni^{58}, Ni^{60}, Ni^{62}) bombarded by 42 MeV alpha particles has been continued, and the program has been extended to include the nuclei of Co^{59}, Cu^{63}, Cu^{65}, Nb, Rh, Pd, and Pt. The proton detector, a scintillation dE/dx - E telescope, and the particle identification system have been described previously.[1,2]

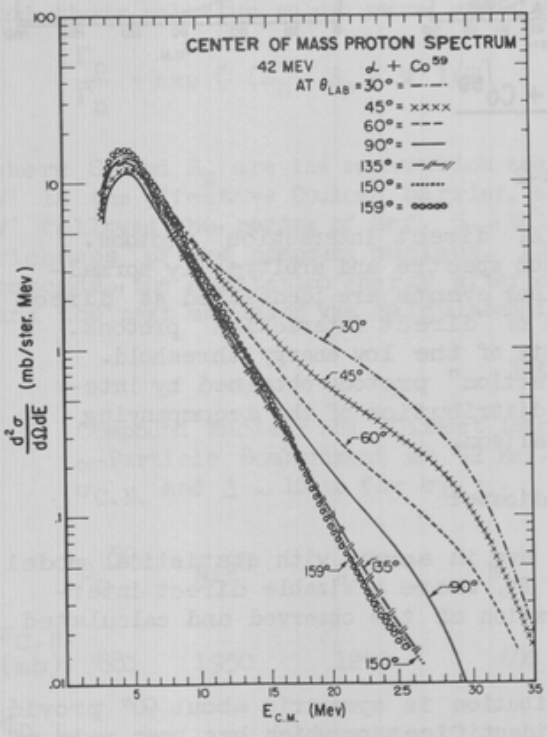

Fig. 14-1

Proton spectra from Co^{59} at various angles. The spectra shown are points.

The energy and angular distributions are similar in general character to the distributions for Co^{59} shown in Fig. 14-1. The energy distributions have been compared to predictions based on the statistical theory. As has been widely found in comparable experiments,[3] a large fraction of the yield in medium-weight isotopes can be attributed to compound nuclear processes. The remainder of the yield is attributed to direct interaction processes. Thus, the term "direct interaction" is used here to represent the entire nonstatistical yield.

To put the assignment of compound and direct parts of the energy distribution on a quantitative basis, a calculation was performed of the expected evaporation spectrum, according to the statistical theory. Details of this calculation are described below. The observed and calculated spectra were normalized at an intermediate energy. Invaribly, the observed yield exceeded the calculated yield at higher energies. This excess is designated here the "direct interaction" component as in Fig. 14-2(a) and plots of its spectra for Co^{59} are shown in Fig. 14-2(b). Once this designation is made, based on energy distributions alone, an integration over energy gives total compound and direct yields at each angle (see Fig. 14-2(c)). The results can be summarized in terms of angular distributions and total proton yields (see Table 14-1).

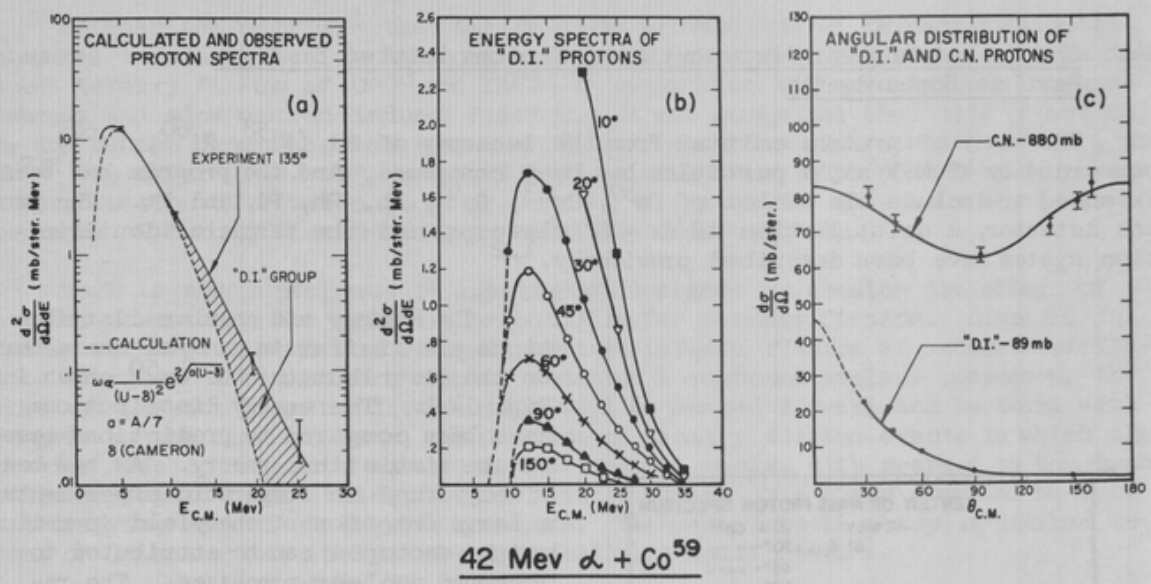

Fig. 14-2

Energy spectra and angular distributions of "direct interaction" protons. (a) The differences between observed proton spectra and arbitrarily normalized calculated spectra for compound nuclear events are identified as "direct interaction" protons. (b) Energy spectra of "direct interaction" protons. The dashed segments reflect the uncertainty of the low energy threshold. (c) Angular distribution of "direct interaction" protons obtained by integrating the spectra of (b). The angular distribution of the accompanying compound nuclear events is shown for comparison.

Preliminary analysis of the results indicate:

(a) The compound nuclear proton yields are in accord with statistical model predictions, with the possible exception of Pt, where a sizable direct interaction component makes unambiguous normalization of the observed and calculated spectra difficult.

(b) The compound nuclear angular distribution is symmetric about 90° providing independent evidence in support of the identification which has been made of compound nuclear events.

(c) The direct interaction yield is approximately the same for all targets (~85 mb), although the yield for Ni^{58} is slightly higher than for the other targets.

(d) The direct interaction angular distribution is forward peaked. However, a sizable component is observed at 90° (~ 3 mb/steradian) and there is a noticeable direct interaction yield even at 150°.

Taken together, the results of (c) and (d) indicate that it is difficult to learn about statistical compound nuclear processes from the study of proton spectra in heavy nuclei. Here neutron evaporation dominates the compound nuclear events and proton distributions are severely contaminated by noncompound nuclear events, even at backward angles.

The statistical model calculation of the expected spectrum, mentioned above, uses a computer code to follow the cascade of protons and neutrons. The spectral shape is governed by the value of $E\sigma_c\omega(U)$ where E is the emitted nucleon energy, σ_c the cross section for the inverse reaction, and $\omega(U)$ the level density of the residual nucleus at an excitation energy U. An analytic expression fit to Shapiro's[4] continuum theory calculation was used for the proton σ_c (with r_o = 1.5 f) and σ_c for neutron emission was assumed constant. The level density used was of the form $\omega(U) = (\text{const.}/U^2) \exp 2\sqrt{aU}$.

The relative emission probabilities of protons (Γ_p) and neutrons (Γ_n) were assumed to add to one (i.e., zero probability for other than nucleon emission), and their relative values were given by the expression

$$\frac{\Gamma_p}{\Gamma_n} = \exp\left[(S_n - S_p - V')/T\right]$$

where S_n and S_p are the separation energies of neutrons and protons respectively, V' is the effective Coulomb barrier, and T is the nuclear temperature. Values of V' followed the recipe of Ref. 5. Values of $S_n - S_p$ were based on the "proton-richness" of the compound nucleus. (See, for example, Ref. 6.) In trailing the cascade, the excitation energy after each emission was divided into one-MeV bins, and the next emission was calculated from this distribution of excitation energies.

Table 14-1

Compound Nuclear and "Direct Interaction" Proton Yields Following α-Particle Bombardment at 42 MeV. Preliminary Errors are $\sim$ 10% for $\sigma_{C.N.}$ and $\pm \sim$ 10 mb for $\sigma_{D.I.}$.

	C_o^{59}	Ni^{58}	Ni^{60}	Ni^{62}	Cu^{63}	Cu^{65}	Rh	Pt
$\sigma_{C.N.}$ (mb)	880	1950	1240	690	900	500	270	50*
$\sigma_{D.I.}$ (mb)	89	116	94	89	75	75	94	

*The value for Pt is the total yield.
(R. West)

---

1 Cyclotron Research, University of Washington (1962), p. 34.
2 Cyclotron Research, University of Washington (1961), p. 53.

3 See, for example, N. O. Lassen and V. A. Siderov, Nucl. Phys. 19, 579 (1960).
4 M. M. Shapiro, Phys. Rev. 90, 171 (1953).
5 I. Dostrovsky, Z. Frankel and G. Friedlander, Phys. Rev. 116, 1082 (1962).
6 D. Bodansky, R. K. Cole, W. G. Cross, C. R. Gruhn, and I. Halpern, Phys. Rev. 126, 1082 (1962).

15. Study of Low Energy Particle Evaporation

Work is continuing towards the study of barrier penetration by low energy protons which are emitted in compound nuclear de-excitation cascades. In particular, detection equipment is being developed for the following purposes: (1) measurements of proton emission spectra, down to proton energies of 1 MeV, (2) a coincidence study of energy correlations between emitted protons, with emphasis on the low energy protons, and (3) a coincidence study of energy correlations between emitted protons and gamma rays. The coincidence experiments serve to test the usual assumption that the very low energy protons and the gamma rays are emitted at the end of the cascade at excitations which do not exceed substantially the threshold for neutron emission.

The detection systems require low threshold energies, unambiguous rejection of undesired particles (including high energy protons which pass through the detectors) and, at least for the coincidence experiments, large areas. Details of the equipment being developed are presented in Sec. 26 and 27. (D. Bodansky, E. R. Parkinson, and B. J. Shepherd)

16. Analysis of Continuous Gamma Ray Spectra

In the measurement of a gamma-ray spectrum, complications in obtaining the true gamma energy distribution from the observed pulse height distribution arise from the necessity of "unscrambling" the contributions of gamma rays of widely varying energy. These complications are especially severe in the study of continuum gamma spectra, as are found in compound nuclear reactions.[1]

Among the complications are: the straightforward but numerous arithmetic manipulations implicit in solving many equations in many unknowns, the experimental difficulty of measuring the response function of the spectrometer with good accuracy over a large range of gamma energies, and the very fundamental difficulty arising from the degeneration of the data by the combination of finite resolution and statistical fluctuations. The unscrambling process may magnify such fluctuations into severe errors.

In order to learn about the importance of these problems, and their implications for the choice of equipment, a variety of calculations have been made with the IBM 709 computer at the University of Washington computer facility. A computer program using an iterative technique for spectrum unfolding[2] has been modified for use at this laboratory. Since direct unfolding calculations, involving the inversion of the spectrometer response matrix, yield more explicit estimates[3] of the errors of the unscrambling process than is the case with

iterative calculations, matrix inversion calculations have been performed with the object of comparing the usefulness of data obtained with scintillation crystals of varying sizes.

Specific results depend greatly upon the energy range of interest, the number of channels of information desired, the number and distribution of total counts, and special characteristics of individual spectrometers, such as degree of collimation of the beam striking the scintillator. For the situation of interest, namely, the energy range 0.5 to 8.5 MeV, 20-channel sampling of data, and a spectral distribution dropping rapidly and uniformly with energy, it was found that for a two-inch by two-inch scintillation crystal, counting statistical errors were magnified by factors of the order of a thousand or more to give intolerable errors in the upper channels of unscrambled data. In general, rapid improvements from the effect of improved photopeak-to-total counts ratio result from even moderate increases in size, and a four-inch by four-inch crystal could be expected to worsen statistics by less than a factor of ten in the same situation. (E. R. Parkinson)

---

1 See the experimental discussion in Sec. 18 of this report.
2 J. F. Mollenauer, U.C.R.L. Technical Report UCRL-9748, August, 1961.
3 R. E. Rand, Nucl. Instr. Methods 17, 65 (1962).

---

17. Angular Distributions of Neutrons in Bombardments with 42 MeV Alpha Particles

The neutron time-of-flight spectrometer has been used during the past year with only the following rather minor changes:

(1) The stilbene crystal has been replaced by a plastic scintillator. The plastic is less fragile and has a slightly faster decay time than stilbene. The pulse shape method of distinguishing pulses caused by neutrons from those caused by gamma rays, although useful for background studies, proved to be unnecessary when taking data.

(2) The distance from the target to the detector has been increased from 173 cm to 206 cm. This longer flight path makes it possible to take data at 30°, whereas 45° was the most forward angle at which data could be taken previously.

Preliminary data were reported last year[1] on the angular and energy distributions of neutrons emitted from Al, Co, Nb, and Au in bombardments with 42 MeV alpha particles. These data have been extended to include 30° in the laboratory system. The energy range has also been increased and now includes neutrons with energies as high as 14 MeV.

The final results for spectra and angular distributions of neutrons from the four targets studied are given in Fig. 17-1. The results are plotted as a function of angle in the center-of-mass system, and they are labeled by neutron energy in MeV, also in the c.m. system. Where it is possible, the data are fit by a

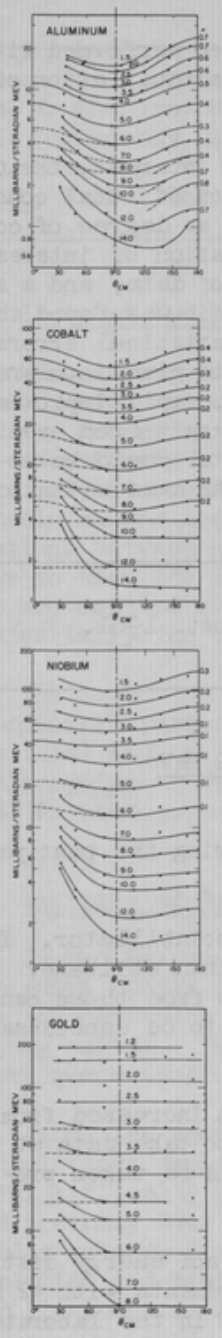

Fig. 17-1(a,b,c,d)

Angular distributions of neutrons from the alpha particle bombardment of (a) aluminum, (b) cobalt, (c) niobium, (d) gold.

curve of the form $(1 + a \cos^2\theta)$, and the value of a is recorded at the right of each curve.

The general features of the preliminary distributions were discussed in the 1962 progress report, and that discussion is still applicable to the data shown in Fig. 17-1.

Further analysis of the data was done in terms of four rather distinct aspects of compound nucleus theory. These are:

(1) Total neutron production cross section.

(2) Level density parameters as determined from back angle spectra.

(3) Nuclear moments of inertia as determined by the anisotropies.

(4) Shape and magnitude of the "direct interaction" component of the continuous spectra.

Some of the results of this analysis are presented in Table 17-1 on the following page.

The total neutron production cross sections are in reasonable agreement with expectations, with the possible exception of aluminum which seems rather small.

The level density parameters agree with values measured by others with different techniques. There are two values listed in Table 17-1 for the ratio of the nuclear moment of inertia to the rigid body moment of inertia. The purpose of this is to show that the moment of inertia varies with excitation energy. Nuclei with large amounts of excitation energy contribute relatively more neutrons to the higher energy part of the neutron spectrum than do nuclei with small amounts of excitation energy. The values in the table indicate that, as the excitation energy increases, the moment of inertia approaches the rigid body value.

Angular and energy distributions have also been taken in alpha particle bombardments of three zinc isotopes, Zn^{64}, Zn^{66}, and Zn^{68}. These data have been analyzed only in terms of total neutron production cross section. The measured cross sections from Zn^{64}, Zn^{66}, and Zn^{68} are 1.4, 2.3, and 3.2 Barns respectively. The ratio of these yields has been compared to predictions based on the analysis of Bodansky[2] concerning the

Table 17-1

	Total Neutron Production Cross Section (barns)	Level Density Parameter "a" (MeV^{-1})	Ratio of Nuclear Moment of Inertia to Rigid Body Moment of Inertia		Estimate of Total Amount of Direct Interaction Neutrons (barns)
			E_n = 2MeV	E_n = 4MeV	
Aluminum	0.9	2.6	0.7	1.0	0.10
Cobalt	2.6	7.4	0.5	0.85	0.15
Niobium	5.1	8.9	0.5	0.7	0.23
Gold	6.2	22.5			0.15

relative probability of neutron and proton emission, and the agreement is fairly good. (D. Drake, I. Halpern, and R. Parkinson)

---

1 Cyclotron Research, University of Washington (1962), pp. 31, 32.
2 D. Bodansky, Ann. Rev. Nucl. Sci., 12, 99 (1962).

---

18. Gamma Rays from Compound Nuclear De-excitation

An excited compound nucleus most probably will decay by particle emission as long as this process is energetically possible. In general, several MeV of excitation energy remain after the particle emission cascade has been completed, and the nucleus then completes its de-excitation by gamma decay. These gamma rays are of interest in the study of angular momentum effects. Much of the initial angular momentum remains after all particles have been emitted. The effects of this residual angular momentum are reflected in the angular distribution of the gamma rays, the number of gamma rays emitted per reaction, and their energy spectra.

Preliminary results on the angular distribution of gamma rays were obtained in the process of collecting data for the neutron evaporation experiment. (See Sec. 17.) Some of the tentative conclusions reached from these runs, carried out with a plastic scintillator, are: (1) The angular distributions of gamma rays from Al, Co, Nb, and Au are not very markedly anisotropic; (2) the mean energy of the gamma rays decreases as A increases; and (3) in bombardment of three zinc isotopes, Zn^{64}, Zn^{66}, and Zn^{68}, it was found that the ratios of the number of gamma rays from the Zn^{66} and Zn^{68} bombardments to the Zn^{64} bombardments were 1.17 and 1.21, respectively.

A 4" by 4" NaI(Tl) crystal was used in a second experimental arrangement that was designed especially to study gamma ray emission. The NaI(Tl) counter was more efficient and had better resolution than the plastic used in the neutron

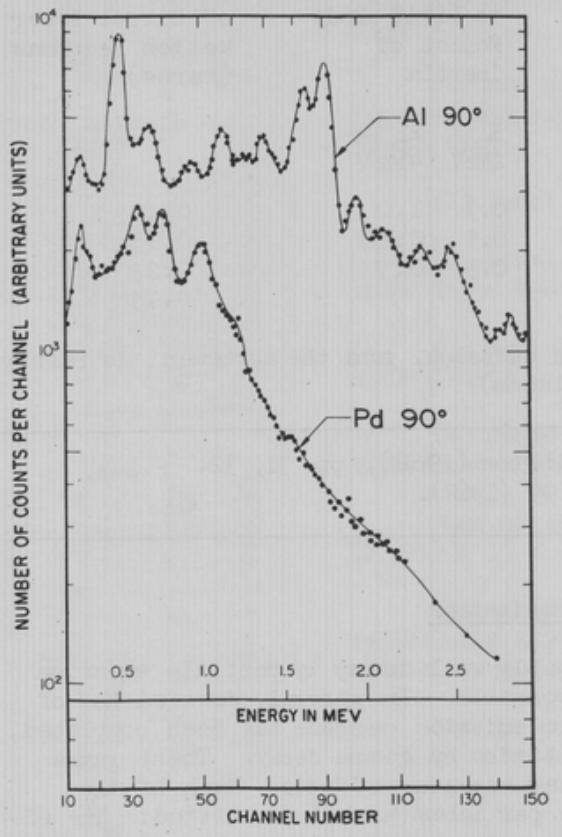

Fig. 18-1

Pulse height spectrum of gamma rays from the alpha particle bombardment of aluminum and of palladium at 90°

experiment. However, due to the slower decay time of NaI, it was more difficult to separate gamma rays and neutrons by time-of-flight.

Gamma rays from bombardments of several elements (Al, Co, Nb, Au, Zn^{64}, Rh, Pd) were studied with the use of this NaI crystal. The raw data from all bombardments except that of gold show evidence of peaks in a predominantly continuous spectrum. Fig. 18-1 shows the 90° gamma spectra from the aluminum and palladium bombardments. Through an "unfolding" procedure which corrects for the complicated response of a scintillation crystal to gamma rays, these pulse-height spectra will in principle yield gamma-ray energy spectra. (See Sec. 16.) Only very preliminary measurements have been made of gamma-ray angular distributions, and consistent results have not yet been obtained.

It is planned to continue this work with an improved detection system. The counter will be moved farther away from the target to eliminate neutron contamination; an anti-coincidence annulus counter is to be used to facilitate unfolding of the measured spectra. (D. Bodansky, D. Drake, I. Halpern, E. R. Parkinson, B. J. Shepherd, and C. F. Williamson)

V. MISCELLANEOUS NUCLEAR REACTIONS

19. The T(d, n) He^4 Reaction at 21 MeV

The angular distribution in the d + T → He^4 + n reaction for deuteron energies to about 14 MeV,[1] and polarization of outgoing neutrons for deuteron energies to about 8 MeV[2] have been carefully measured. This reaction at increased energies is expected to shed some light on the reaction mechanism (the small angle part of the angular distribution was well fitted by stripping curves). It is also of interest because of possible use as a strong source of monoenergetic high energy (also polarized) neutrons.

Preliminary work on this reaction has been done with deuterons of 21 MeV incident upon a Ti - T target on 0.002 in. stainless steel backing. Neutrons at forward angles (θ_{lab} = 9.5°, 11.5°, 16.5°, and 21.5°) were detected with a recoil proton plastic scintillation counter. Because of their high energy (up to 36 MeV) recoil proton pulses were expected to rise high above the background. However, the stainless steel backing (both the tritium and blank target) produced a high background, apparently due to the Co^{59}(d, n) reaction. Only the upper part of spectrum showed neutrons from tritium, allowing only a limited accuracy of determination of relative cross sections at various angles. The following improvements will be attempted: (1) a stilbene scintillator (2 in. dia. by 2 in.) with pulse-shape particle gamma ray discrimination, (2) the time-of-flight technique to separate neutrons from gamma rays, and (3) a gaseous tritium target. (J. Alster, D. Garreta, K. Ilakovac, C. F. Williamson)

---

1 L. Stewart, J. E. Brolley, Jr., and L. Rosen, Phys. Rev. 119, 1649 (1960).
2 R. B. Perkins and J. E. Simmons, Phys. Rev. 124, 1153 (1961).

---

20. Investigation of (α, Be^8) Reactions

Further work has been carried out on the detection of (α, Be^8) reactions in which the Be^8 nuclei are detected by observing small angle coincidences between the break-up alpha particles.[1] The present investigations have been concerned mainly with the reaction Mg^{24}(α, Be^8) Ne^{20} leading to the ground state of Ne^{20}. For a bombarding energy of 42 MeV the Be^8 nuclei emitted at forward angles have a kinetic energy large compared with their break-up energy, and thus the alpha particles are confined to a narrow energy band and to a narrow cone in space. For example, at θ_{lab} = 20° the Be^8 has an energy of 31.0 MeV. The alpha particles have energies from break-up of 13.8 to 17.2 MeV and are contained within a cone of 6.3° full angle. Thus to detect the Be^8 one can impose strict energy requirements and also demand that the coincident alpha particles be within 6° of each other.

In the initial phase of this experiment, the two alpha particles were detected with scintillation counters. These proved to be unsatisfactory, however, because of their poor energy resolution and the apparently rather low cross section for the Mg^{24}(α, Be^8) Ne^{20} reaction. Therefore, a counter arrangement consisting of two surface barrier solid state detectors is now being used. The

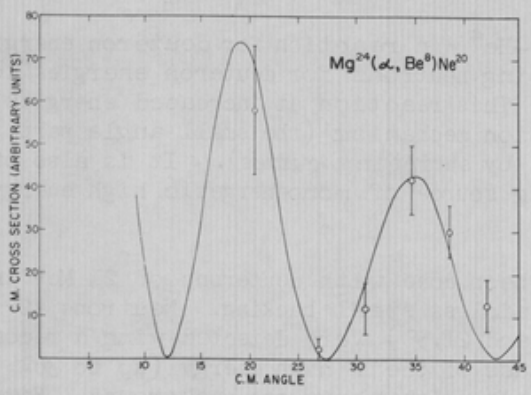

Fig. 20-1

Measured angular distribution for $Mg^{24}(\alpha, Be^8)Ne^{20}$ reaction, taken with 42 MeV alpha particles. The solid curve is proportional to $(P_{11}(\cos\theta))^2$. The differential cross section at the highest peak (near 20°) is roughly 60 microbarns/steradian.

pulses from each detector are routed to separate inputs of a fast-slow coincidence system, and the coincidence output pulse is used to gate a 32 by 32 two-dimensional pulse height analyzer. The Be^8 events correspond to a line of constant total energy on the two-dimensional display. Such a line, at the correct energy, stood out clearly above background events at the peaks of the angular distribution (see Fig. 20-1), but less clearly elsewhere. As a check on the identification of the events, it was verified that the "Be^8 line" disappeared when the detectors were separated by more than the cone angle.

The results obtained to date are shown in Fig. 20-1. The cross section is low, roughly 60 microbarns/steradian at the maximum. The angular distribution shows indications of an oscillatory behavior. Comparison is made to an arbitrarily normalized plot of $(P_{11}(\cos\theta))^2$, whose theoretical justification is given below.

The angular distribution for an (α, Be^8) reaction joining the ground states of two even-even nuclei has a particularly simple general form. All particles involved have zero spin; consequently the orbital angular momentum ℓ in the incoming channel equals the orbital angular momentum in the outgoing channel, while the projection of orbital angular momentum along the beam direction is zero in both channels. Therefore the angular distribution may be written

$$\frac{d\sigma}{d\Omega} = \frac{1}{4k_o^2} \sum_{\ell=0}^{\infty} \left| (2\ell + 1)\, S_\ell\, P_\ell\, (\cos\theta) \right|^2$$

where S_ℓ is the reaction matrix element, $S^J_{\ell I;\ell' I'}$, for the special case $I = I' = 0$.

Various theoretical models can be used to evaluate the reaction matrix elements. For example, in the zero-range distorted-wave Born approximation the matrix elements are proportional to overlap integrals of the product of radial wave functions for the projectiles in appropriate optical potentials. The main characteristics of the observed angular distributions can probably be understood, however, without recourse to such specific calculations, and indeed it is quite possible that the distorted-wave model does not furnish a correct detailed description of the reaction.

The crucial features of any specific direct interaction model are that the largest reaction matrix elements correspond to "grazing" collisions with orbital angular momenta of the order of a critical angular momentum, L = kR, and that there is a coherence between these matrix elements. Let us therefore assume merely that these qualitative features characterize the reaction matrix elements. At small angles the Legendre polynominals of neighboring ℓ are nearly equal, and the cross section then has the approximate form

$$\frac{d\sigma}{d\Omega} = C\, P_L{}^2 (\cos\theta)$$

This expression motivates the solid curve (L = 11) shown in Fig. 20-1, but the fit obtained must be viewed with caution in view of the limited amount of data presently available. It is interesting to note, however, that L = 11 is less than the value of critical angular momentum which is obtained for the alpha particle-Mg^{24} interaction from analysis of elastic alpha particle scattering, namely L = 15; further, it is less than what would be inferred for the final Be^8 - Ne^{20} interaction (where the relative wave length is almost the same as the reduced alpha particle wave length).

It is possible that the rather small cross section observed implies a small reduced width of Mg^{24} for dissociation into an alpha particle and the ground state of Ne^{20}. In view of our lack of knowledge of the reaction mechanism, however, this conclusion is clearly premature.

It is planned to extend the present measurements on Mg^{24}, and also to investigate other target nuclei. Use of the new degrader system (see Sec. 23) may permit a study of the energy dependence of the reaction. (J. S. Blair, D. Bodansky, R. E. Brown)

---

1 Cyclotron Research, University of Washington (1962), p. 38.

---

21. Deuteron and Alpha Particle Pickup Reactions

Following a suggestion of D. H. Wilkinson, a study of (d, Li^6) reactions has been begun in an attempt to detect α-particle clustering on the surface of intermediate weight nuclei. Particles were detected with a proportional dE/dx counter used in conjunction with a solid state E counter. Particle identification was accomplished by means of an electronic stretcher and x - y oscilloscope system described in last year's report.[1] Angular distributions of lithium nuclei from the Ni(α, Li^6) Co and V(α, Li^6)Ti reactions were measured to determine whether these reactions were best represented in terms of a compound nuclear or a direct reaction picture. The strong forward peaking of the detected Li particles and lack of symmetry about 90° in the center of mass system suggest that the direct model with the interaction localized on the surface of the target nucleus is the appropriate one here. We have succeeded in detecting lithium nuclei from (d, Li) reactions on targets of Ni, Zn, Cu, Mg, and Al with incident deuterons of 21 MeV energy. (P. Mizera, F. Slee, and C. Zafiratos)

---

1 Cyclotron Research, University of Washington (1962), p. 39.

22. Angular Distributions of Fast Neutrons in Alpha Particle Bombardments

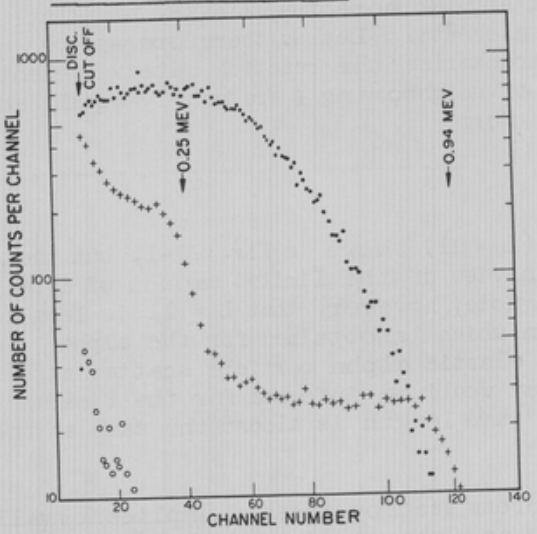

Fig. 22-1

C^{11} positron spectrum. The dots represent positrons from the decay of C^{11} in a crystal exposed to neutrons from the alpha particle bombardment of Mg. The circles represent typical background. The crosses represent a Na^{22} calibration spectrum.

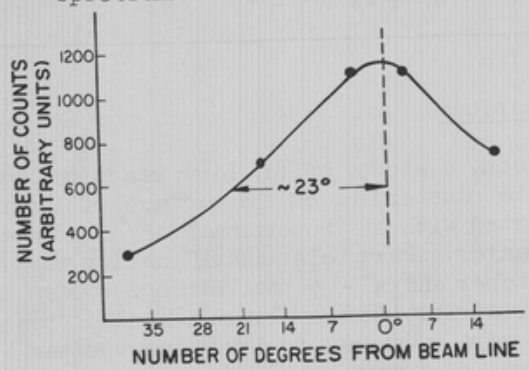

Fig. 22-2

Angular distribution of fast neutrons from the alpha particle bombardment of Cu. The left-hand scale is proportional to the total amount of C^{11} formed in the bombardment of each crystal.

The experimental work on the angular distributions of fast neutrons, measured by threshold detectors, has been completed. Due to background troubles, the use of copper as a detector was discontinued, and this report concerns only data obtained with C^{12} detectors.

The carbon detectors were NE 102 plastic scintillators,[1] that were arranged outside a small scattering chamber.[2] Targets located at the center of this scattering chamber were bombarded with about two microamperes of alpha particles for twenty minutes. Some of the neutrons produced in this bombardment form C^{11} in the scintillators by the reaction $C^{12}(n, 2n)C^{11}$. After a bombardment, the plastic scintillators were mounted on a photomultiplier, and the twenty-minute C^{11} activity was measured. In this way the carbon serves as its own detector, eliminating the need for a Geiger counter or second crystal.

Fig. 22-1 shows the C^{11} decay spectrum, a Na^{22} gamma spectrum which was used for calibration, and a background spectrum, measured with a crystal that had not been exposed to the neutron flux.

Fig. 22-2 shows the angular distribution of fast neutrons from the alpha particle bombardment of copper. Similar curves were obtained for the other elements that were used as targets. The forward peaking can be understood on the basis of a simple model in which the incident alpha particles produce neutrons as they strike the target nucleus. The strong absorption of alphas by nuclei together with the moderate absorption and refraction of neutrons give rise to the focusing.

Fig. 22-3 shows the half widths of the angular distributions for various targets as a function of A. The half widths of the heavier elements ($A \geq 63$) appear to be nearly constant. This is attributed to the competition between the "defocusing effect" of the Coulomb field and the increased focusing due to the larger nuclear radius, as A is increased.

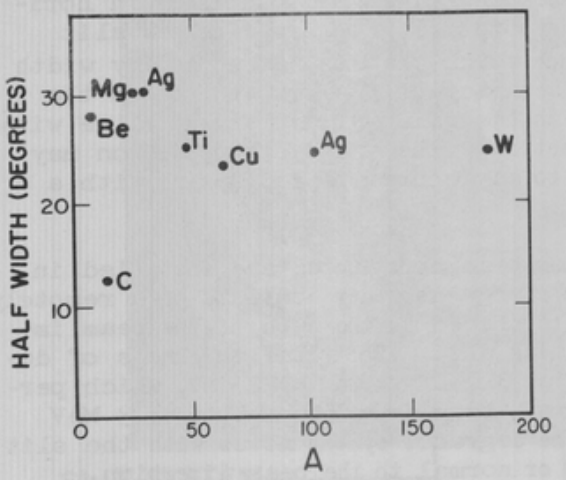

Fig. 22-3

Half widths of angular distributions of fast neutrons vs. A.

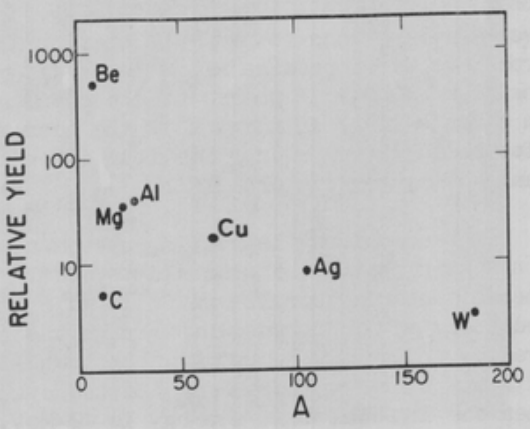

Fig. 22-4

Relative yields of fast neutrons vs. A.

Fig. 22-4 shows that the relative yields of high energy neutrons decrease as A increases. This might be expected because the neutrons have to travel farther inside the nucleus and are likely to lose too much energy in collisions with other nucleons.

For light nuclei where the level spacing is large, structure effects can become important. Carbon, for example, with a very small half width and low yield, seems to be an exception to any general conclusions one might draw from these data. (D. Drake, I. Halpern, E. Henley)

---

1 The use of these detectors was suggested to us by Dr. R. B. Day.
2 This chamber was kindly loaned to us by the Los Alamos Scientific Laboratory.

VI. ACCELERATOR RESEARCH AND DEVELOPMENT

23. New Slit and Beam Energy Degrader System

The beam defining slit system, which is located between the focusing and analyzing magnets, has been rebuilt in order to increase the precision in horizontal beam location and definition at this point (Fig. 23-1). The new slit system allows one to set the opening through which the beam passes at any width from zero to approximately one cm with an accuracy of ± 0.1 mm and to set the position of the midpoint of the opening with the same accuracy at any valve within a range of 9 cm normal to the beam direction. The slit system position may also be adjusted along the beam direction to an accuracy of ± 0.05 in. with a range of approximately 6 in.

A beam-energy degrading system also has been constructed and installed in conjunction with the new slit system. The energy degrader consists of a remotely operable set of beryllium foils which may be placed in the path of the beam immediately after it passes through the defining slit. The total thickness of degrading foils may be varied continuously from 0.001 in. to 0.022 in., which permits one to vary the energy of the cyclotron α beam from 25.6 MeV to 41.3 MeV when the initial beam energy is 42 MeV. The degrader system moves with the slit system when it is moved either parallel to or normal to the beam direction. There is a Faraday cup incorporated into the system which may be flipped in and out of the beam in order to monitor the beam current through the slits and degrader foils. (T. J. Morgan)

24. Van de Graaff Accelerator Program

The Van de Graaff accelerator building plans were completed and submitted for bids in July, and at the September 28, 1962, meeting of the Board of Regents, contracts were awarded for the construction of the building. The final total budget for the building was $1,082,617 with the National Science Foundation providing $500,000 and the University of Washington providing the remainder.

Construction was started early in November, 1962, and is scheduled for completion by November 1, 1963.

In the meantime, the National Science Foundation has made an additional grant of $2,040,500 for completion of the project. This grant included the $500,000 mentioned above for the building. Contract negotiations were completed with High Voltage Engineering Corporation for the remainder of the equipment to be furnished by them in order to complete the installation of the three-stage accelerator system.

The tandem stage and other auxiliary equipment necessary to its operation and use as a research tool are to be shipped by December, 1963, and are scheduled to be in operation by May, 1964. The injector stage is to be shipped in May, 1964, and should be in operation before the end of that year.

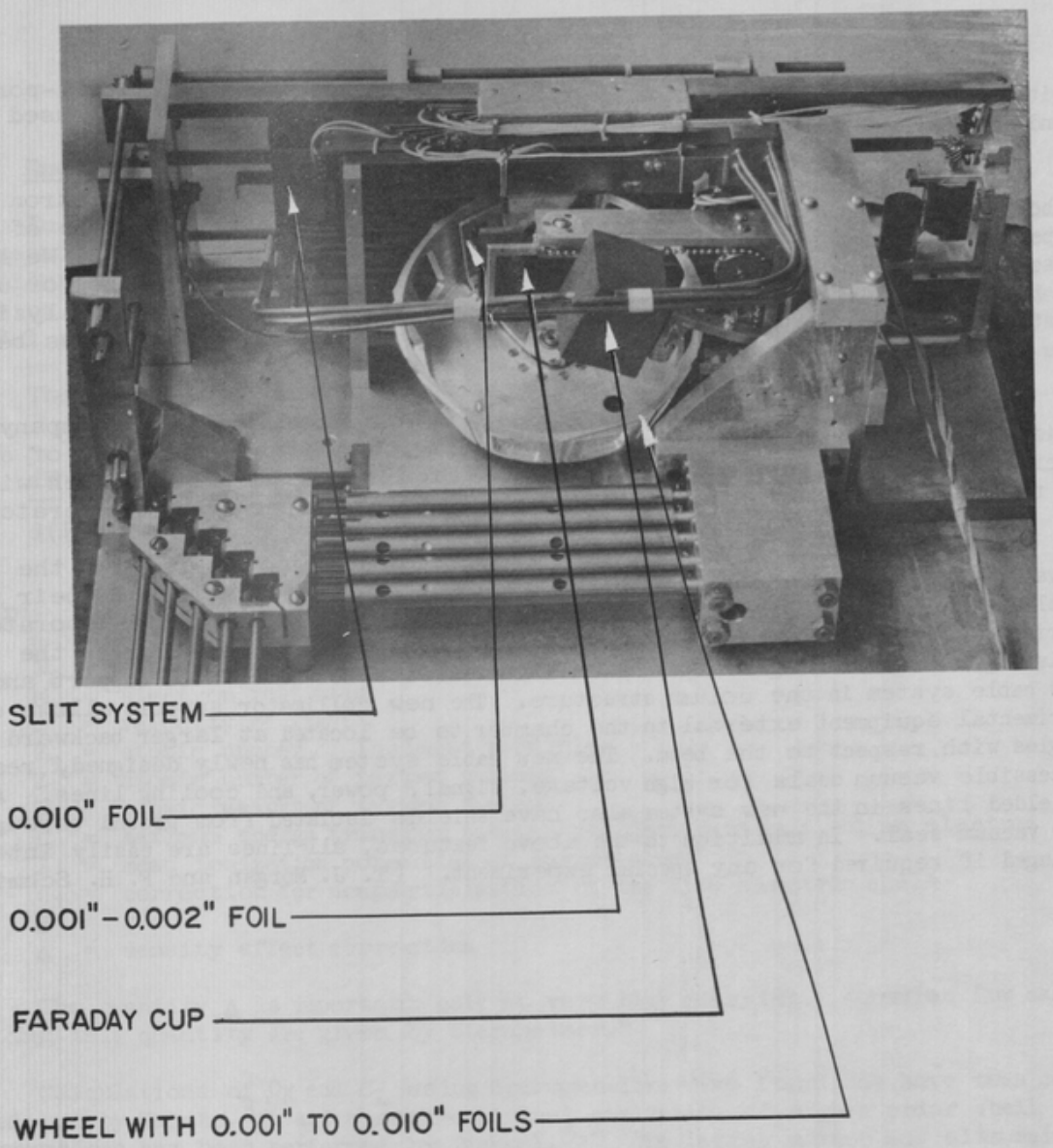

Fig. 23-1

Degrader and slit system.

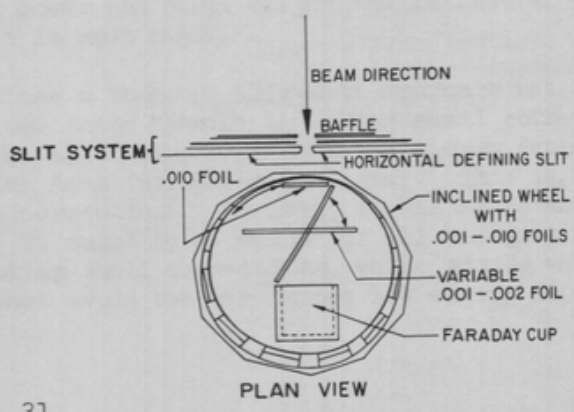

The equipment to be delivered with the tandem stage includes a seven-port switching magnet and a total of four beam tube extensions which will be used to conduct the beam to the experimental targets.

An improved version of the 60" scattering chamber used in the cyclotron laboratory is being constructed and will be ready for installation in one of the experimental areas of the Van de Graaff building by the spring of 1964. We have also succeeded in procuring a surplus navy gun mount of sufficient size for use as the support and rotational structure for a heavy particle momentum analysis system. This structure had to be moved into one of the experimental caves before the walls were completed, as it was too large to go through the doors.

Negotiations also have been completed with Air Reduction Pacific Company, which supplies liquid nitrogen to the University, for a storage facility of sufficient capacity to supply the 220 liters of liquid nitrogen per day which will be required for operation of the vacuum system for the three-stage accelerator.

Construction of the Van de Graaff accelerator building has required the removal of the cyclotron cooling towers from their original location and their installation in an area immediately north of the existing hot chemistry laboratory. During the shut-down of cyclotron operation necessitated by this change, the existing 60" scattering chamber has had installed a new collimator support and a new cable system in the column structure. The new collimator support allows experimental equipment external to the chamber to be located at larger backward angles with respect to the beam. The new cable system has newly designed, readily accessible vacuum seals for high voltage, signal, power, and cooling lines. All shielded lines in the new system also have shields isolated from ground through the vacuum seal. In addition to the above features, all lines are easily interchanged if required for any special experiment. (T. J. Morgan and F. H. Schmidt)

VII. INSTRUMENTATION FOR RESEARCH

25. Energy Loss Calculations for Charged Particles

In view of the increasing tendency in this laboratory toward automatic data processing, the need was felt for a series of computer subroutines to give corrections for energy loss of charged particles. In addition, an empirical correction was sought for the Bethe[1] stopping power relation that would give a meaningful extrapolation to zero energy, allowing the direct calculation of ranges.

The Bethe stopping power relation is usually written in the form:

$$\frac{dE}{d(PX)} = \frac{2n^2 e^4 N_o Zi^2}{M_o c^2 \beta^2} \frac{Z}{W} \left\{ \log \left[\frac{2M_o c^2 \beta^2 H}{I^2(1-\beta^2)} \right] - \beta^2 - \frac{2}{Z} \sum_i c_i - \Delta \right\}$$

where

e = electronic charge
N_o = Avogadro's number
M_o = electron rest mass
c = velocity of light
Z_i = atomic number of incident particle
Z = atomic number of target nucleus
W = atomic weight of target nucleus
H = maximum energy transfer between incident particle and an electron
I = mean ionization potential of target atoms
c_i = correction for nonparticipation of the i'th electron shell
β = v/c
Δ = density effect correction

The quantity Δ is important only at very high energies. Formulas for calculating this quantity are given by Sternheimer.[2]

Calculations of C_K and C_L using hydrogen-like wave functions have been carried out by Walske,[3,4] and a semi-empirical evaluation of higher order shell corrections has been performed by Bichsel.[5,6] The latter author has also made extensive calculations of the stopping power and range of protons in several elements, obtaining very good agreement in most cases.

In the present series of calculations a somewhat different approach was taken. Instead of seeking to correct the Bethe formula by adding shell corrections, it was decided to seek a function that would duplicate the energy dependence and perhaps the Z-dependence of the mean ionization potential. This is, of course, analagous to finding the shell corrections. However, it has an advantage in that, if the correct form is found, it ought to be valid for all energies. On the other hand, the technique of adding shell corrections, while giving very good agreement at higher energies, cannot avoid the very grave low energy difficulties of the Bethe formula.

The procedure was thus to express the mean ionization potential as

$$I = I(E_i, Z)$$

with E_i as the incident particle energy. The functional form was sought on a purely empirical basis. The one finally adopted is

$$I(E_i, Z) = I_o Z \exp(1/Z) \tanh^2\left\{\sqrt{B(E_i)}\right\} \times \left\{1 - a \exp(-b/E_i)\right\} \left\{1 - 0.5\,\delta\,(Z_i - 1)\right\}$$

where

$$B(E_i) = \left[\frac{2M_o c^2 \beta^2 H}{(1 - \beta^2)}\right]^{1/2} \cdot \frac{1}{I_o Z \exp(1/Z)\{1 - 0.5\,S\,(Zi - 1)\}}$$

and I_o, a, and b are adjustable parameters.

A brief indication of the motivation behind this equation is in order. The factors

$$I_o Z \exp(1/Z)\left\{1 - 0.5\,\delta\,(Z_i - 1)\right\}$$

seem to give a fairly accurate description of the Z-dependence of the mean ionization potential. The last factor is necessary in order to make the expression valid for hydrogen, which appears to have a much lower I-value than its immediate neighbors.

The factor

$$1 - a \exp(-b/E_i)$$

was included in an attempt to match the apparent decrease of the mean ionization potential at very high energies. Unfortunately, data exist at only a few energies above 29 MeV, so that accurate evaluation of the parameters is impossible, and indeed it is uncertain if the functional form given here is valid. Fortunately, the effect appears to be fairly small.

In addition to making the logarithm term well behaved, it is also necessary to take into account the effective charge of low energy ions. This becomes more important as the atomic number of the incident ion increases and there is a greater probability that the ion will not be completely stripped of all its electrons. Fairly extensive measurements of the effective charge of heavy ions in various materials have been made by Northcliffe,[7] and an empirical equation for the effective charge as a function of ion velocity is given in this reference. The formula given by Northcliffe has the disadvantage of bad behavior at low energies; therefore, a functional form was sought which would give good agreement with the data and have "good" behavior at low energies. The form finally adopted was

$$Z_i = Z_o \tanh\left(\frac{C\beta}{Z_o}\right)$$

where

Z_i = effective charge of incident ion
Z_o = atomic number of incident particle
C_o = adjustable parameter

This equation is not dependent upon the atomic number of the target material. Only a few cases have been studied, but it appears from these meagre data that the effective charge is independent of the stopping material.

For the maximum energy transfer, H, the limit for heavy incident particles was taken, i.e.,

$$H = \frac{2M_o c^2 \beta^2}{1 - \beta^2} \cdot \frac{1}{1 + (2M_o/M_i)(E_i/M_i c^2)} \qquad (M_i \gg M_o, \text{ any. E.}).$$

Therefore, the present programs are not valid for electrons and positrons, although they could be modified for light particles by taking the proper form for H.

The values of the four adjustable parameters that were finally chosen are: I_o = 11.6 eV; a = 0.15; b = 100 MeV; c = 172 $\simeq$ (4/π)137.

Having obtained an equation for dE/d(PX), one can in principle obtain the range from

$$R(E_i) = \int_o^{E_i} \left(\frac{dE}{d(PX)}\right)^{-1} dE$$

In actual practice the range must be calculated by numberical integration. In this case the infinity at zero energy can be very troublesome; therefore, the integration is usually begun at some very low energy value, say, 0.001 MeV. The resulting error is completely negligible.

Two programs for the IBM 709 computer have been based upon these formulas. The first makes up tables of range and dE/d(PX) as a function of the incident particle energy. Tables 25-1 and 25-2 give examples of tables prepared for protons on aluminum and gold. The first and last energies in the table and the energy steps between are controlled by the user.

The other program, which is really the one intended for automatic data processing, is a "package" of six function subroutines. These subroutines calculate stopping power, range, emergent energy from an absorber, average angle of deflection due to multiple scattering in an absorber, energy absorbed in the absorber, and thickness of absorber necessary to reduce the incident energy to a given amount.

The last four mentioned subroutines are corrected for multiple scattering by the Fermi[9] formula:

$$\frac{\overline{d\theta^2}}{d(PX)} = \frac{3.55 \times 10^9 \; Zi^2 \; Z^2 \; (1-\beta^2)}{Wi^2 \; W \; \beta^4} \left\{ 16.66 + \log \left[\frac{Wi \; \beta^2}{ZiZ^{4/3} \sqrt{1 - \beta^2}} \right] \right\}$$

where $\overline{\theta^2}$ = root mean square angle of deviation in radians
W_i = mass of incident particle in AMU
W = mass of target nucleus in AMU

and other symbols have already been defined. Here Z_i is taken as the effective charge as defined above.

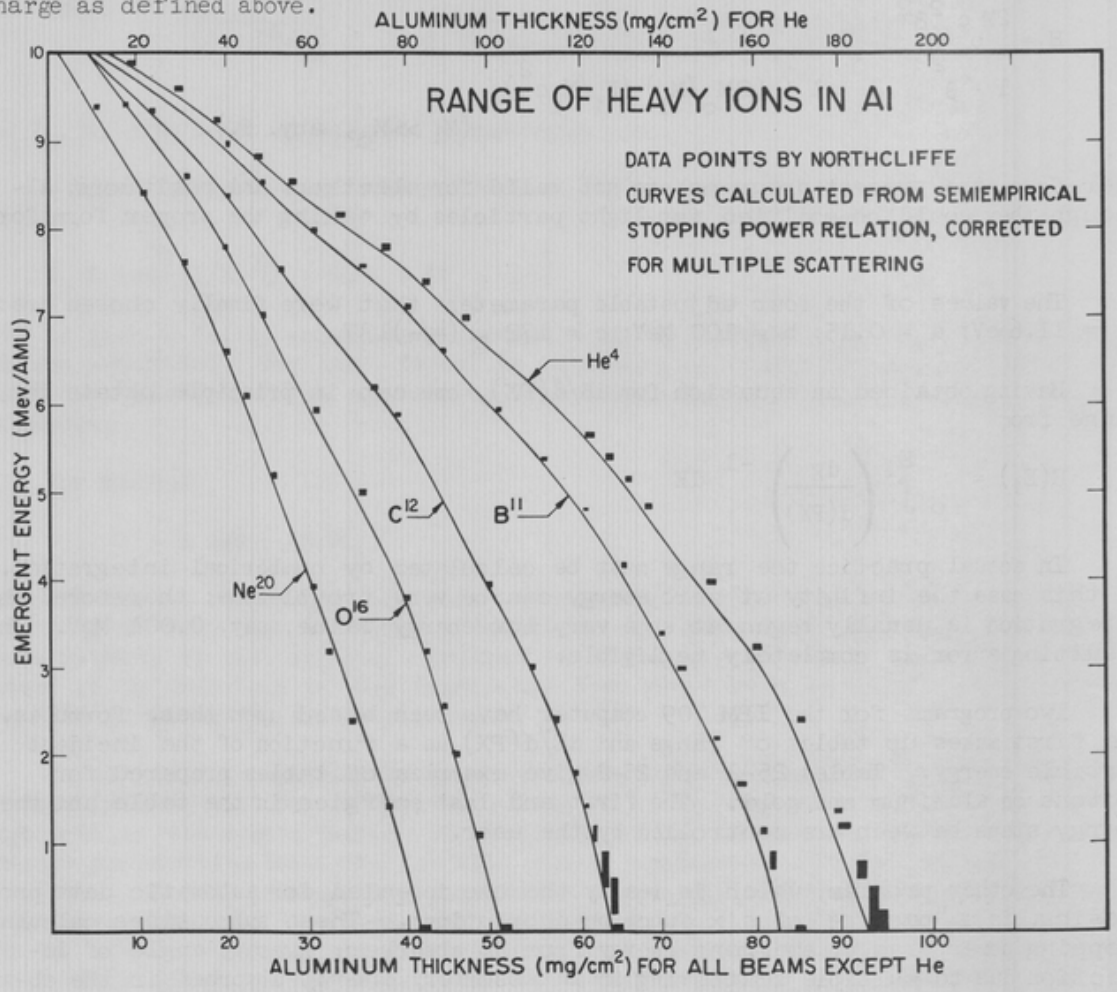

Fig. 25-1

Range-energy relation for heavy ions in aluminum. Solid curves are calculated by methods described in the text. Data points are from reference 7.

TABLE 25-I

PROTONS ON ALUMINUM
ENERGY IN MEV, RANGE IN GM/CM**2, STOPPING POWER IN MEV*CM**2/GM

ATOMIC NUMBER OF INCIDENT PARTICLE = 1.000
ATOMIC MASS OF INCIDENT PARTICLE = 1.008
ATOMIC NUMBERS OF CONSTITUENT ATOMS = 13.000
ATOMIC MASSES OF CONSTITUENT ATOMS = 26.970
ATOMS PER MOLECULE = 1.000

ENERGY	RANGE	STOPPING POWER
0.050	1.853E-04	4.377E 02
0.100	2.990E-04	4.287E 02
0.150	4.194E-04	3.969E 02
0.200	5.494E-04	3.667E 02
0.250	6.898E-04	3.405E 02
0.300	8.405E-04	3.181E 02
0.350	1.001E-03	2.987E 02
0.400	1.173E-03	2.817E 02
0.450	1.354E-03	2.668E 02
0.500	1.545E-03	2.537E 02
0.600	1.955E-03	2.313E 02
0.700	2.404E-03	2.130E 02
0.800	2.890E-03	1.976E 02
0.900	3.412E-03	1.846E 02
1.000	3.969E-03	1.734E 02
1.500	7.269E-03	1.343E 02
2.000	1.138E-02	1.108E 02
2.500	1.627E-02	9.490E 01
3.000	2.190E-02	8.337E 01
3.500	2.825E-02	7.458E 01
4.000	3.530E-02	6.763E 01
5.000	5.142E-02	5.729E 01
6.000	7.016E-02	4.993E 01
7.000	9.144E-02	4.440E 01
8.000	1.152E-01	4.007E 01
9.000	1.413E-01	3.659E 01
10.000	1.698E-01	3.371E 01
11.000	2.006E-01	3.130E 01
12.000	2.337E-01	2.924E 01
13.000	2.690E-01	2.746E 01
14.000	3.065E-01	2.591E 01
15.000	3.462E-01	2.454E 01
16.000	3.880E-01	2.332E 01
17.000	4.319E-01	2.223E 01
18.000	4.780E-01	2.125E 01
19.000	5.260E-01	2.037E 01
20.000	5.762E-01	1.956E 01
29.000	1.116E 00	1.459E 01
300.000	6.555E 01	2.792E 00
615.000	2.027E 02	2.027E 00

TABLE 25–2

PROTONS ON GOLD
ENERGY IN MEV, RANGE IN GM/CM**2, STOPPING POWER IN MEV*CM**2/GM

ATOMIC NUMBER OF INCIDENT PARTICLE = 1.000
ATOMIC MASS OF INCIDENT PARTICLE = 1.008
ATOMIC NUMBERS OF CONSTITUENT ATOMS = 79.000
ATOMIC MASSES OF CONSTITUENT ATOMS = 197.200
ATOMS PER MOLECULE = 1.000

ENERGY	RANGE	STOPPING POWER
******	*****	******** *****
0.050	1.149E-03	7.527E 01
0.100	1.782E-03	8.021E 01
0.150	2.401E-03	7.972E 01
0.200	3.026E-03	7.829E 01
0.250	3.664E-03	7.669E 01
0.300	4.314E-03	7.509E 01
0.350	4.978E-03	7.353E 01
0.400	5.657E-03	7.204E 01
0.450	6.349E-03	7.062E 01
0.500	7.056E-03	6.926E 01
0.600	8.511E-03	6.672E 01
0.700	1.002E-02	6.437E 01
0.800	1.159E-02	6.222E 01
0.900	1.321E-02	6.022E 01
1.000	1.488E-02	5.837E 01
1.500	2.404E-02	5.079E 01
2.000	3.446E-02	4.515E 01
2.500	4.610E-02	4.078E 01
3.000	5.891E-02	3.728E 01
3.500	7.287E-02	3.439E 01
4.000	8.793E-02	3.198E 01
5.000	1.213E-01	2.814E 01
6.000	1.589E-01	2.522E 01
7.000	2.005E-01	2.292E 01
8.000	2.461E-01	2.104E 01
9.000	2.955E-01	1.949E 01
10.000	3.486E-01	1.818E 01
11.000	4.054E-01	1.705E 01
12.000	4.659E-01	1.607E 01
13.000	5.298E-01	1.522E 01
14.000	5.973E-01	1.446E 01
15.000	6.681E-01	1.378E 01
16.000	7.424E-01	1.317E 01
17.000	8.199E-01	1.263E 01
18.000	9.007E-01	1.213E 01
19.000	9.848E-01	1.167E 01
20.000	1.072E 00	1.125E 01
29.000	1.995E 00	8.626E 00
300.000	1.019E 02	1.835E 00
615.000	3.080E 02	1.360E 00

This series of subroutines has been tested by calculating the range-energy relation of heavy ions in aluminum and mylar. These are shown in Figs. 25-1 and 25-2 along with the data of Northcliffe[7] and of Schambra, Rauth, and Northcliffe.[8] The agreement, while not perfect, is judged to be satisfactory in view of the uncertainties involved in calculating ranges for heavy ions. (C. F. Williamson)

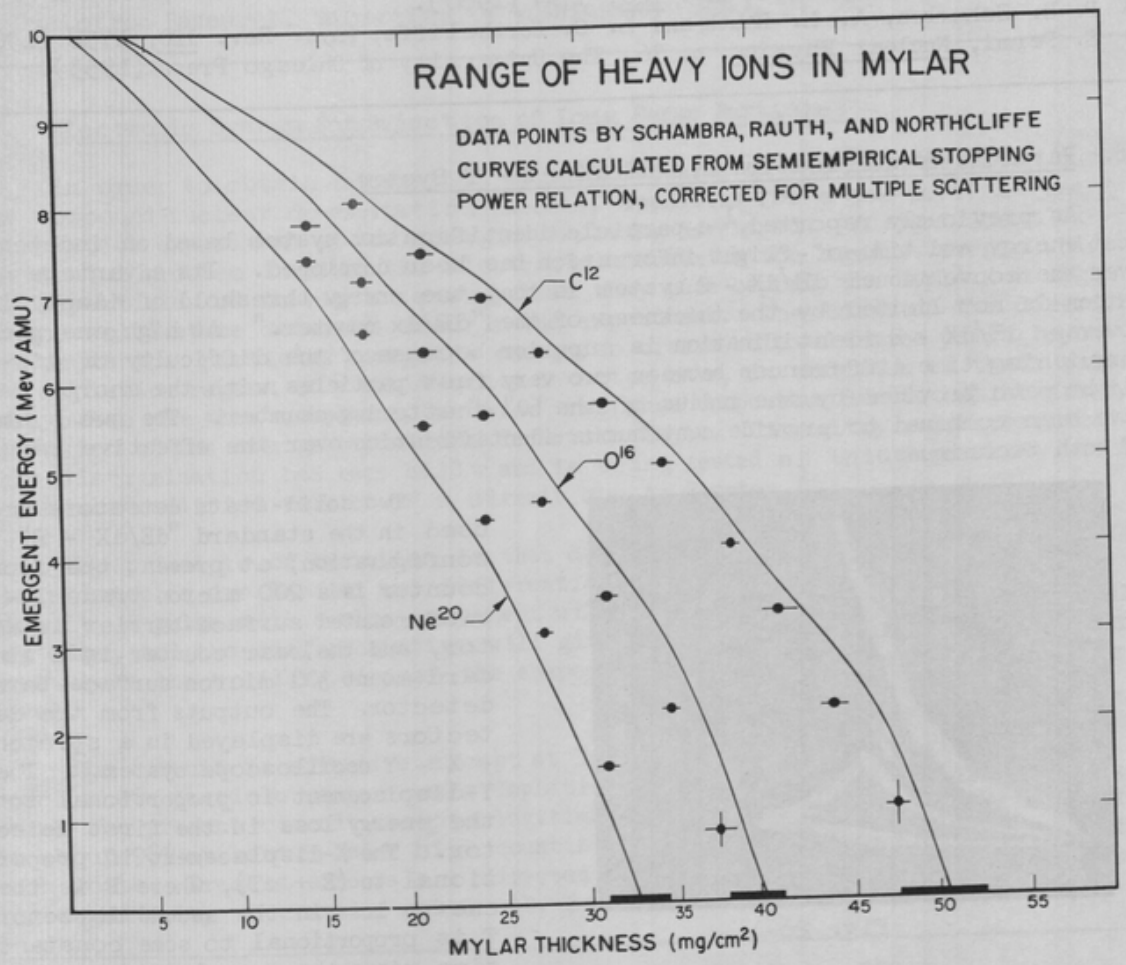

Fig. 25-2

Range-energy relation for heavy ions in mylar. Solid curves are calculated by methods described in the text. Data points are from reference 8.

---

1 H. A. Bethe, Z. Physik 76, 293 (1932).
2 R. M. Sternheimer, Phys. Rev. 103, 511 (1956).
3 M. C. Walske, Phys. Rev. 88, 1283 (1952).
4 M. C. Walske, Phys. Rev. 101, 940 (1956).

5 H. Bichsel, Technical Report No. 3, Linear Accelerator Group, Department of Physics, University of Southern California, Los Angeles 7, California (unpublished).
6 H. Bichsel, Appendix to Technical Report No. 3, Linear Accelerator Group, Department of Physics, University of Southern California, Los Angeles 7, California (unpublished).
7 L. C. Northcliffe, Phys. Rev. 120, 1744 (1960).
8 P. E. Schambra, A. M. Rauth, and L. C. Northcliffe, Phys. Rev. 120, 1758 (1960).
9 E. Fermi, Nuclear Physics, p. 36, The University of Chicago Press (1955).

---

26. Particle Identification in a dE/dX - E - T System

As previously reported,[1] a particle identification system based on independent energy and time-of-flight information has been developed. Its advantage over the conventional dE/dX - E system is that the energy threshold of identification is not limited by the thickness of the "dE/dx counter." At high energies, however, dE/dX - E identification is superior because of the difficulty of distinguishing time differences between two very fast particles with the short flight path provided by the radius of the 60" scattering chamber. The two systems have been combined to provide continuous identification over the effective range of both techniques.

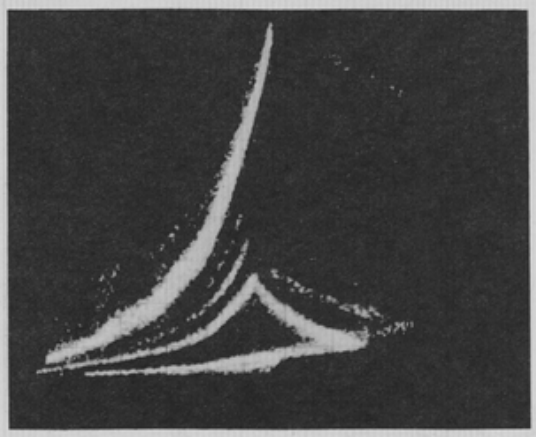

Fig. 26-1

Time exposure of X-Y oscilloscope display of dE/dX vs. (E+cT) for reaction products of 42 MeV alpha particle bombardment of teflon, $(CF_2)_x$. The band corresponding to protons lies lowest, with deuterons, combined tritons and He^3, and alpha particles (in ascending order) in the separated bands above. The folding back of the curves is caused by particles too energetic to stop in the second counter.

Two solid-state detectors are used in the standard "dE/dX - E" configuration; at present the front counter is a 200 micron transmission-mounted surface-barrier detector, and the rear counter is a standard mount 300 micron surface-barrier detector. The outputs from the detectors are displayed in a stretcher - X - Y oscilloscope system.[2] The Y-displacement is proportional to the energy loss in the first detector. The X-displacement if proportional to (E + cT), where E is the energy loss in the second detector, T is proportional to some constant time minus the actual time-of-flight, and c is constant. With this system, one obtains families of curves like those shown in Fig. 26-1.

Particles which do not penetrate into the second counter will fall into one of the rising curves in the left half of the display; very fast particles, which penetrate both counters and give essentially constant "T" pulses, trace out the

familiar family of dE/dX vs. E curves on the right. Gating is accomplished by the now standard technique of observing the masked oscilloscope face with a photo multiplier tube, which gives pulses whenever a spot appears on the uncovered area of the oscilloscope tube face. (D. Bodansky and E. R. Parkinson)

1 Cyclotron Research, University of Washington (1962), p. 29.
2 Cyclotron Research, University of Washington (1961), p. 51.

27. Electronic System for Rejection of Long Range Particles

In order to obtain information about the course of particle emission during the compound-nuclear de-excitation cascade, apparatus for a two-particle energy correlation experiment at low energies is being developed. A significant experimental problem involves the electronic discrimination against events which yield particles of so high an energy that they pass beyond the depletion region of the solid-state detectors used in the experiment. The basis of the discrimination is that particles energetic enough to create hole-electron pairs beyond the depletion region of a solid-state detector have, in addition to their primary fast pulse rise time component, a "slow" response component due to collection by diffusion of the charge beyond the depletion layer. Circuitry which performs this discrimination has been built and is being tested at this laboratory; it is a somewhat modified version of a circuit due to Funsten.[1]

The principle of operation is that delay-line shaped pulses from the solid-state detector are limited and differentiated. With proper adjustment of the circuit, a pulse with a slow component will have a pulse with a very flat trailing edge, and the differentiation will give no output, in contrast to the normal case where the trailing edge of the shaped pulse will drop sharply back to zero level.

The circuit is effective except at low energies and in a region near the point where particle range equals depletion layer thickness. The efficiency with which the present circuit accepts legitimate pulses and rejects "passthru" pulses is about 98% at best. Under high counting rate conditions, the efficiency gets much worse. Present efforts are directed toward improving efficiency and reducing sensitivity to counting rate. (D. Bodansky and E. R. Parkinson)

1 H. O. Funsten, I.R.E. Trans. Nuc. Sci., NS-9, No. 3, p. 190.

28. Gas Targets

The 1 in. diameter gas target described in last year's report was modified several times. The original target had 1/2 mil mylar windows that were damaged by the beam. This problem was overcome by constructing a target in which the beam entered through a thin Ni foil and left through a strip of Ni glued to the mylar window. Counting rates were very low at the 1/2 atmosphere pressure used, so a window that would withstand more pressure was desired. An all foil windowed

target was made using 0.093 mil "Havar"[1] glued to the existing brass frame, which allowed pressures up to three atmospheres to be used. (R. E. Brown, I. Naqib, and D. Shreve)

---

1 Supplied by Hamilton Watch Company.

---

29. Design and Development of Electronic Equipment

Construction of electronic equipment during the past year has been directed towards meeting the needs of current experiments, towards placing the second cyclotron counting area into operational usefulness, and towards preparing for the experiments with the tandem Van de Graaff accelerator. Many of the new units built for cyclotron use during the past year are viewed as prototypes of units to be used with the tandem. In addition, a limited number of chassis have been build or are under construction, which are already designated for the tandem counting areas.

Specific items of electronic equipment include:

(1) A transistorized triple fast coincidence system has been completed. It has several desirable features which the original vacuum tube version did not have.[1] The coincidence resolving time can be adjusted by an external cable to times ranging from four nanoseconds to several microseconds. The coincidence scheme is the triangular configuration discussed in the earlier report, but a new limiter is used in front of the coincidence circuit itself. Facility is provided for the single pulses to be scaled.

(2) The extensive use of oscilloscope XY display techniques for particle identification has led to the construction of a revised linear pulse stretcher.[2] In addition to stretching the pulses, the unit establishes coincidence criteria for controlling the oscilloscope intensification. The newer unit gives improved performance at both the low energy and the high energy end points, and handles pulses over a dynamic range of more than one hundred.

(3) The fraction of data collected that is processed through the computer has been increasing to such extent that we now rent an IBM-870 system to convert data from punch paper tape to punched cards. Careful error checking is necessary with this type of data collection. We have designed and constructed a parity checker which is inserted between the N. D. 120 and the tape perforator. The unit will detect errors in parity from the analyzer itself. It also turns on a warning light if there is a tape advance signal without a punch command. This latter trouble has occurred occasionally.

(4) The multichannel analyzer output usually presents the nonsignificant zeros in the typed data. The typewriter zero key wears badly and becomes slow in operation. We have designed and constructed a relay network which channels the leading or nonsignificant zeros to the space solenoid until a nonzero digit appears. This transfers the significant zeros to the zero solenoid. At the next space command the system is reset to suppress leading zeros again. The data on a

typed sheet are more easily read and analyzed, and the peaks are much easier to spot.

(5) Several panel mount hybrid millimicroammeters were designed and constructed. The unit works on a single source of power, is stable, and can be used for measuring currents of 10^{-11} amperes to 10^{-6} amperes by switching external resistors. The entire circuitry is contained in a printed circuit card mounted on the rear of a 3-inch 0-1 milliampere meter. It uses a Raytheon CK 5886 electrometer tube with grid currents of 10^{-12} amperes or less.

(6) An eight-channel pulser has been designed and constructed. It is intended to facilitate pre-testing of complex electronic arrangements, involving both fast and slow coincidence systems. The unit has four fast and four slow outputs, which are time coincident to within one nanosecond. They may be positive or negative, over amplitudes from 0.1 to 10 volts. The fast pulses have a 3-nanosecond rise time and a 40-nanosecond duration. The slow pulses have either 100-nanosecond or 200-nanosecond risetimes and 5-microsecond or 100-microsecond decay times, respectively. The repetition rate is continuously variable from 55 pulses per second to 10,000 pulses per second. All outputs can drive 125 ohm coaxial lines.

(7) A spectrum generator, which can give randomly spaced pulses, has been designed and constructed. The amplitudes are varied by a linear ramp. The noise generator is a gas tube; all the rest of the circuitry is transistorized. The unit is used to test the equality of width of the channels of a multichannel analyzer. The unit has two linear ramps with separate coincident outputs which make it useful for two dimensional analyzer testing.

(8) To collect data more effectively from complex coincidence experiments, we have designed and constructed two electronic chassis to control the logic for the multichannel analyzer routing signals. One device provides routing signals for the simultaneous accumulation of two gated and two ungated spectra, when used with the ND 501 dual buffer storage system. The other device scales the ungated spectra by factors of 10, 20, or 40, when both gated and ungated spectra are being simultaneously accumulated, to reduce dead time losses.

(9) A two-channel time-to-pulse-height converter is being constructed. It is specifically intended for use in coincidence experiments, in which time-of-flight information is obtained for two particles. Coincident events, in this arrangement, will be events for which there are simultaneous "stop" pulses (from the cyclotron r.f.), rather than simultaneous pulses in the two detectors. This avoids difficulties from differing flight times.

(10) All components of the two-dimensional 256-channel analyzer have been transistorized. The main effort during the past year has been devoted to building and debugging the arithmetic scaler system and the readout system. Readout modes now available are: (a) a one-dimensional oscilloscope display of pulse height spectra, (b) a punch paper tape tally of counts per channel, and (c) an intensity modulated two-dimensional oscilloscope display of counts per channel. The system can now receive and read out data as a one-dimensional analyzer, but there is cross talk in the two-dimensional data collecting mode. Work is in progress to correct this malfunctioning.

(11) Construction for the new tandem Van de Graaff has been concentrated so far on a scaler system. Standard printed circuit cards have been developed for scalers, scaler power supplies, and a master scaler controller. Assembly of chassis from these cards is proceeding.

(12) Additional chassis which have been designed and constructed for current use include: two limiter shapers and pulse height converters for time-of-flight work, a three-channel coincidence unit, a dual variable delay unit, a dual linear gate, several preamplifiers, special photomultiplier bases, and power supplies for use with solid state detectors and preamplifiers.

(13) Equipment purchased commercially includes: a Nuclear Data ND 150 FM multichannel analyzer, a Tally tape perforator, a Tally tape reader, a Tally tape-to-typewriter converter, two Tektronix type 503 oscilloscopes for use with the multichannel analyzers, a Tektronix type RM 541 A oscilloscope for use in the second counting area, three 0 - 3 kv regulated power supplies, an RIDL Nuvistor preamplifier, four Cosmic double delay line linear amplifiers, a Cosmic coincidence system, and an air conditioning unit for cooling counting room equipment. In addition, an IBM 870 system has been rented and is in operation at the cyclotron. (D. Bodansky; L. H. Dunning; H. Fauska, Senior Physicist, Research Electronics Supervisor; R. E. Karns, Jr.; R. A. Matthews; R. McCleary; R. L. McKenzie; G. C. Monge; N. G. Ward)

---

1 Cyclotron Research, University of Washington, 1960, p. 43.
2 Cyclotron Research, University of Washington, 1961, p. 51.

VIII. APPENDIX

30. Statistics of Cyclotron Operation

The disposition of the time available for cyclotron operation during the period from May 16, 1962, to May 15, 1963, is given in Tables 30-1, 30-2, and 30-3, which are self-explanatory.

Table 30-1 Division of Cyclotron Time Among Activities

Activity	Time	
	Hours	Per Cent
Normal Operation	3774	68.7
Setup of Experiments	337	6.1
Cyclotron Testing	163	3.0
Scheduled Repairs and Modifications	416	7.6
Unscheduled Repair	305	5.5
Failure of Experimental Equipment	50	0.9
Unsatisfactory Cyclotron Operation	125	2.3
Experiments Using No Beam	98	1.8
Unrequested Time	207	3.8
Visitors	16	0.3
	5491	100.0

Table 30-2 Division of Normal Operation Time Among Normal Facilities

Projectiles	Time	
	Hours	Per Cent
Alpha Particles	2772	73.4
Protons	927	24.6
Deuterons	75	2.0
	3774	100.0

31. Bombardment for Outside Investigators

During the year bombardments were requested by and performed for a number of outside investigators. These are summarized in Table 31-1.

Table 31-1 Bombardment for Outside Investigators

Investigator	Time	
	Hours	Per Cent
Boeing Airplane Company	4	12.9
University of Colorado	7	22.6
Western Washington College of Education	17	54.8
University of Oregon	3	9.7
	31	100.00

32. Cyclotron Personnel

Faculty

David Bodansky, Associate Professor
Arthur W. Fairhall, Associate Professor
George W. Farwell, Professor
James B. Gerhart, Associate Professor
I. Halpern, Professor
Ksenofont Ilakovac, Visiting Associate Professor
Fred H. Schmidt, Professor

Cyclotron Research Staff

Jonas Alster, Research Assistant Professor
Francis Bartis, Research Instructor[1]
Ronald E. Brown, Research Assistant Professor
Darrell M. Drake, Research Instructor[2]
Ted J. Morgan, Research Associate Professor; Supervisor, Nuclear Physics Laboratory
Isam M. Naqib, Research Instructor[3]
Claude F. Williamson, Research Assistant Professor
Chris Zafiratos, Research Instructor[4]

Pre-Doctoral Associates

Joseph A. Coleman[5]
David L. Hendrie
Wojctech A. Kolasinski
E. Roland Parkinson
Gurnam S. Sidhu
Frederick W. Slee
Richard W. West

Research Assistants

Physics

Nelson Cue
Ann F. Ehrke[6]
Lawrence B. Fogdall[6]
Thomas D. Hayward
Joseph S. Heagney
Paul Mizera
Daniel Montague
Roy J. Peterson
Joseph E. Ramus[6]
Barry J. Shepherd
David C. Shreve
Edward B. Warren
David Yu[6]

Chemistry

Walter Loveland
Paul Gudiksen[6]

Full-Time Technical Staff

Machine Shop

Harvey E. Bennett, Foreman
Norman E. Gilbertson
Charles E. Hart
Floyd E. Helton
Gustav E. Johnson
Ed P. McArthur
Bernard Miller, Assistant Foreman
Byron A. Scott
Allen L. Willman

Electronic and Electrical

Laverne H. Dunning
Robert B. Elliott
Harold Fauska, Senior Physicist, Research Electronics Supervisor
Russell E. Karns
Rex McCleary[6]
Robert L. McKenzie[6]
Richard A. Matthews[6]
George C. Monge
John W. Orth, Assistant Supervisor, Nuclear Physics Laboratory
George E. Saling
Norman G. Ward

Design and Drafting

Robert G. Clarke
Peggy Douglass
Dolores Lenhart
James Miles[6]
Peter Momcilovich, Engineer
Lewis A. Page

Accelerator Operators

Barbara J. Barrett
Georgia Jo Rohrbaugh

Others

Vida F. Drummond, Secretary[6]
Tylaine Hansen, Office Assistant
Kyum Ha Lee, Film Scanner
Diana Marshall, Secretary
Ann Rutter, Secretary[6]
Joanne M. Sauer, Radio Chemist
Harriet Wasserman, Radio Chemist[6]

Part-Time Technical Staff

Student Helpers

Chung-Wu Ho[6]
Makoto Hori
Kent McLean
Carol Lewis Ming
Tamae Sato
Harry Winsor[6]
Akiko Yamanouchi

Others

Gloria Marks, Clerk Typist[6]
Don A. Miller, Stores Manager

---

1 Now at Physics Department, Indiana University, Bloomington, Indiana.
2 Now at University of Illinois, Urbana, Illinois.
3 Now at Florida State University, Tallahassee, Florida.
4 Now at Los Alamos Scientific Laboratory, Los Alamos, New Mexico.
5 Now at Princeton University, Princeton, New Jersey.
6 Terminated.

33. Advanced Degrees Granted, Academic Year 1962-1963

Francis J. Bartis: Ph.D. An Investigation of the Decay of Carbon - 10 by Means of a New Type of Toroidal Spectrometer.

Joseph A. Coleman: Ph.D. Two Studies of Fission Phenomena at Moderate Energies.

Darrell M. Drake: Ph.D. A Study of Neutron Evaporation in 42 MeV Alpha Particle Bombardment of Several Elements.

Lawrence Fogdall: M.S.

Paul Mizera: M.S.

Daniel G. Montague: M.S.

Isam M. Naqib: Ph.D. Excitation of Nuclear Levels in Mg^{24}, Al^{27}, and C^{12} Through Inelastic Scattering of Alpha Particles.

Barry J. Shepherd: M.S.

34. List of Publications

The following articles, originating in this laboratory, were published during the year ending June 15, 1963:

"Ranges of Be^{9} Ions in Al and Au," C. O. Hower and A. W. Fairhall, Phys. Rev. 128, 1163 (1963).

"Fission Product Yields in Helium-Ion Induced Fission of Au^{197}, Pb^{204}, and Pb^{206} Targets," E. F. Neuzil and A. W. Fairhall, Phys. Rev. 129, 2705 (1963).

"Energy Levels in N^{14} Pertaining to the Ratio C^{12}/C^{13} Produced in the CNO Cycle," R. E. Brown, Astrophys. J. 137, 338 (1963).

"Alpha-Gamma Angular Correlations and the Distorted-Waves Theory," D. K. McDaniels, D. L. Hendrie, R. H. Bassel, and G. R. Satchler, Physics Lett. 1, 295 (1962).

"Background Reduction in Nuclear Reaction and Scattering Experiments by Means of a Cyclotron-D Voltage Regulator," F. H. Schmidt, H. Fauska, and J. W. Orth, Nuclear Electronics III, International Atomic Energy Agency (Vienna), 1962.

"Compound Statistical Features in Nuclear Reactions," David Bodansky, Annual Reviews of Nuclear Science, Vol. 12, p. 79 (1962).

The following abstracts orginating in this laboratory were published during the year ending June 15, 1963:

"8 Decay of Carbon 10 and the Cluster Model of the Nucleus," F. J. Bartis, Bull. Am. Phys. Soc. 7, 461 (1962).

"Ternary Fission at Moderate Excitation Energies," J. A. Coleman, A. W. Fairhall, and I. Halpern, Bull. Am. Phys. Soc. 7, 471 (1962).

"Mass-Yield Curves in Symmetric Fission," A. W. Fairhall, Bull. Am. Phys. Soc. 7, 491 (1962).

"Two New Energy Levels in the Al^{27} Nucleus," G. W. Farwell, D. L. Hendrie, and I. M. Naqib, Bull. Am. Phys. Soc. 7, 454 (1962).

"Proton Spin-Flip and Substate Excitation in Inelastic Scattering," F. H. Schmidt, Bull. Am. Phys. Soc. 7, 494 (1962).

"Angular Distributions for C^{12} (α, Li^6) B^{10} and N^{14}(α, Li^6) C^{12}," C. D. Zafiratos, Bull. Am. Phys. Soc. 7, 454 (1962).

"Studies of Neutron Evaporation in 42 MeV α-Particle Bombardment of Several Elements," D. Drake, P. Axel, I. Halpern, and R. Parkinson, Bull. Am. Phys. Soc. 7, 470 (1962).

"Inelastic Scattering of 42-MeV α Particles by Mg^{26} and Al^{27}," I. M. Naqib and G. W. Farwell, Bull. Am. Phys. Soc. 8, 318 (1963).